UNC-WRRI-72-64

ANALOG MODELING TO DETERMINE THE FRESH WATER AVAILABILITY ON THE OUTER BANKS OF NORTH CAROLINA

By

George J. Kriz
Associate Department Head
In Charge of Biological and Agricultural Engineering Extension
North Carolina State University
Raleigh, North Carolina 27607

The work upon which this publication is based was supported in part by funds provided by the Office of Water Resources Research, Department of the Interior, through the Water Resources Research Institute of The University of North Carolina as authorized under the Water Resources Research Act of 1964, with matching funds provided by the Water Resources Research Institute and the North Carolina State University Agricultural Experiment Station.

Project No. B-006-NC
Matching Grant Agreement No. 14-01-0001-1932, F. Y. 1969

April 1972

ABSTRACT

Wise use of the Outer Banks of North Carolina is important to the state and the nation not only for their recreational value, but also for the protection from the open sea their presence affords the mainland. One important component in the wise use of the Outer Banks is the availability of potable water. Although adequate supplies of potable water have been available in the past, an increasing demand for fresh water supplies caused by increasing numbers of tourists and permanent residents requires that maximum withdrawals of potable water be made without destructive pollution of the aquifer by salt water intrusion.

Because field studies are very difficult and time consuming, laboratory experiments were conducted using a Hele-Shaw model to predict maximum safe pumping rates that could be obtained from a horizontal gallery for various soil and rainfall conditions on long oceanic islands. Particular attention was given to obtaining potable water on the Outer Banks of North Carolina.

The Hele-Shaw model was designed and built to represent a cross section of a long oceanic island. The two fluids that simulated fresh water and salt water were obtained by adding a viscosity increasing agent to water. The density of one batch was increased by adding salt and sugar. The "fresh water" was added along the top of the fresh water lens in the model at cyclic time intervals. Fluid was pumped from the fresh water lens through one of three galleries. Two of the galleries were located below mean sea level, and one was located at mean sea level. During a test, pumping from a gallery was initiated at a low rate and

ACKNOWLEDGEMENTS

This report is based on research supported in part by funds provided by the Office of Water Resources Research, Department of the Interior, through the Water Resources Research Institute of The University of North Carolina as authorized under the Water Resources Research Act of 1964, Project Number B-006-NC, Agreement Number 14-01-0001-1932. A special note of appreciation and gratitude is addressed to Professor David H. Howells, Director of the Institute, for his assistance and advice during the course of the study.

Dr. Eugene W. Rochester, a former graduate student in the Department of Biological and Agricultural Engineering, North Carolina State University, was responsible for much of the analog modeling presented in this report. Mr. Thomas V. Honeycutt, undergraduate student in the Department of Biological and Agricultural Engineering, North Carolina State University, was responsible for developing much of the application analyses.

Notes of gratitude are expressed to Messrs. R. C. Heath, E. O. Floyd, M. D. Winner, Jr., District Chief, former Hydraulic Engineer, and Hydrologist, respectively, of the United States Geological Survey for their cooperation in supplying information concerning their research on the Outer Banks, and to Hercules, Incorporated, for supplying gratis much of the cellulose gum used in the laboratory study.

was continued at that rate until equilibrium of the interface was obtained. The pumping rate was increased in increments allowing equilibrium to be reached at each increment until the maximum continuous rate was obtained. Pumping stopped when the free surface was pulled to the top of the gallery or when salt water was pumped into the gallery.

The locations of the free surface and interface were recorded for each pumping rate. The maximum safe pumping rate was related to the rainfall and island conditions and characteristics. All the data are presented graphically in dimensionless form to make them applicable to a wide variety of conditions as well as in tabular and graphical form with dimensions to facilitate their use. Several examples are also included.

The laboratory tests showed that the Hele-Shaw model is a very satisfactory analog to predict the location of the fresh water - salt water interface for a variety of conditions. It was determined that increased pumping rates are possible when a horizontal gallery is located below mean sea level, but the risk of salt water intrusion is greatly increased. A maximum safe pumping rate of at least 50 percent of the recharge parameter after subtracting known losses can be expected from a gallery located at mean sea level.

TABLE OF CONTENTS

LIST OF FIGURES

Page

LIST OF TABLES

SUMMARY AND CONCLUSIONS

The major purposes of this investigation were to determine the suitability of a Hele-Shaw model for studying potable water availability on long oceanic islands, to predict maximum safe pumping rates that avoid dangerous salt water pollution of the fresh water lens, and to predict the approximate location of the fresh water - salt water interface on the Outer Banks of North Carolina under various conditions of infiltration, island characteristics, and pumping.

The Hele-Shaw model proved to be a very satisfactory analog to predict the location of the fresh water - salt water interface under conditions of no pumping, safe pumping rates, and the approximate location of the fresh water - salt water interface except for long intervals between rainfalls, low rainfall intensities, and/or low hydraulic conductivities. Even though the tests were conducted in an environmentally controlled chamber, these latter conditions could not be attained because they required the measurement of extremely small quantities of fluid over long periods of time. It was found that proper combinations of a viscosity improving agent [carboxymethylcellulose (CMC), 7L], salt, sugar, and water produced fluids that had the correct density ratio of fresh water to salt water without appreciably varying the viscosity of either mixture.

Because it is impossible to model the essentially infinite number of natural conditions of varying rainfall intensities and intervals between rainfalls, tests were conducted to determine the effects of

different infiltration rates and frequencies of rainfall applications on the location of the interface under conditions of no pumping. Neither factor was found to have a statistically significant effect.

The depth of the interface appeared to be logarithmically related to the recharge parameter under conditions of no pumping. The recharge parameter is defined as the relative infiltration rate (rainfall intensity divided by hydraulic conductivity) multiplied by the fraction of time that rainfall occurred.

A maximum safe pumping rate of at least 50 percent of the recharge parameter after subtracting known losses such as evapotranspiration can be expected from a gallery located at mean sea level. Increased maximum pumping rates are possible from a gallery located below mean sea level, but the risk of salt water intrusion is greatly increased. Anisotropic conditions affect the positions of the interface and the free surface, but do not affect the maximum safe pumping rates.

Because of the complexity of the system studied in this investigation, no mathematical studies were made, and the investigator knows of no other mathematical developments that were suitable for comparison. No direct comparisons with field data were made because field data presently being collected are from vertical wells, and this investigator knows of no relationship to directly compare data from a vertical well with that from a horizontal well. One set of data from a horizontal pumping test conducted some years ago was inadequate for comparison purposes. However, results from Hele-Shaw model studies for drainage investigations previously conducted in our laboratories were not statistically different from mathematical and field results.

The results of the study are useful to practicing engineers for the following types of problems. The location of the interface for varying amounts of rainfall per storm and periods of time between storms under conditions of no pumping allows upper and lower bounds of the interface to be determined so that a more economical field testing procedure can be developed. The maximum pumping rate from a horizontal gallery located above mean sea level can be determined for a given set of conditions. The effects of various pumping rates on the location of the interface can be studied for a range of rainfall conditions and island characteristics. The effects of soil anisotropy on the location of the interface can be investigated.

Tables and/or figures were developed to facilitate solving the problems listed above. An example of each type of problem is presented in the section entitled "APPLICABILITY OF RESULTS TO LONG OCEANIC ISLANDS".

RECOMMENDATIONS

The following recommendations can be made as a result of this study.

1. Use of a Hele-Shaw model is a very valuable analog in rapidly determining changes in the location of the fresh water - salt water interface for various rainfall and island conditions and characteristics. It does, however, have limitations for certain combinations of conditions.

2. When used with salt, sugar, and water, carboxymethylcellulose (CMC), 7L, is a very good viscosity increasing agent to obtain a suitable fluid to use in the Hele-Shaw model.

3. Horizontal galleries on long oceanic islands should be located at, rather than below, mean sea level to prevent the risk of salt water contamination of the potable water supply.

4. Additional research should be undertaken to:

   a. Determine the locations of the fresh water - salt water interface when the horizontal pumping gallery is located other than at the midpoint of long oceanic islands.

   b. Develop a suitable analog for the combination of rainfall and island conditions and characteristics that cannot be modeled by the Hele-Shaw model.

   c. Compare the results of this study with adequate field data.

   d. Determine the most economical methods of installing horizontal galleries.

   e. Compare the economics of a horizontal gallery versus a vertical well.

INTRODUCTION

North Carolina has over 250 mi of Atlantic coastline, much of which consists of a chain of long, sandy, barrier islands. These islands are separated from the mainland by marshes at some points and by as much as 30 mi of open water at other points. These islands range in width from a maximum of about 3 mi to a minimum of about 1,000 ft. Land surface elevations range from sea level along the beaches and in tidal marshes of Pamlico Sound to about 60 ft above mean sea level on some of the sand dunes. Two of these islands, Hatteras and Ocracoke, and sometimes neighboring islands, are collectively referred to as the Outer Banks. The preservation of these Outer Banks is important to the state and the nation not only for their recreational value, but also for the protection from the open sea their presence affords the mainland.

Potable water on the Outer Banks is obtained either by intercepting rainfall and storing it or by pumping water from shallow wells or infiltration galleries. The wells and galleries pump water from a fresh-water lens which floats on the more dense salt water. However, indiscriminate pumping of this water can result in its pollution by salt water. Adequate supplies of water have been available up to the present time when controlled pumping procedures were applied. However, increased demand on the fresh water supplies caused by increases in numbers of tourists and permanent residents requires that maximum pumping rates be obtained without destructive pollution of the aquifer by salt water intrusion. It appears at the present time that the ultimate use of the Outer Banks will be limited by the availability of potable water rather

than the availability of recreational and residential space.

The principal purpose of this study was to develop an analog model that would complement and supplement the field studies for determining better estimates of safe yield of potable water being conducted by the North Carolina District of the Water Resources Division, United States Geological Survey (USGS). If a model to predict the potable water at a cross sectional area of the Outer Banks could be developed, other areas could easily be modeled in the laboratory and expensive field investigations could be eliminated.

A Hele-Shaw model was used to determine safe pumping rates of potable water for long oceanic islands that have two-dimensional flow characteristics. The pumping rates are related to island size, soil characteristics, infiltration, and gallery location and are presented graphically in dimensionless groupings. Locations of the free surface and fresh water - salt water interface for various pumping rates are presented in dimensionless form to make the data applicable to a wide variety of conditions, as well as in tabular and graphical form with dimensions to facilitate their use. Several examples are included.

OBJECTIVES

The objectives of this investigation concerning withdrawal of potable water on the Outer Banks were as follows:

1. to design and construct a Hele-Shaw model to represent a pre-selected cross sectional area of the Outer Banks;

2. to predict the location of the interface under various conditions of infiltration, island characteristics, and pumping;

3. to determine if the intermittent relative infiltration rate has an important effect on the interface location;

4. to determine if the rainfall frequency has an important effect on the interface location;

5. to predict maximum safe pumping rates that avoid dangerous salt water pollution of the fresh water lens;

6. to compare the laboratory results with on-going field studies; and

7. to present the findings in tabular and/or graphical form so as to extend the results to other long oceanic islands.

REVIEW OF LITERATURE

Groundwater Studies on the Outer Banks

Harris and Wilder (1964) presented a precipitation map showing average annual precipitation to vary from 46 to 55 in. on Hatteras Island. Lloyd and Dean (1968) reported that the highest monthly rainfall on Bodie Island occurs during the months of July, August, and September. The location of the islands is given in Figure 1. E. Tabor (Harris and Wilder, 1964) of the U. S. Weather Bureau at Cape Hatteras stated that rainwater in the area was found to contain as much as 998 ppm (parts per million) chloride. Harris and Wilder (1964) stated that the rainfall is rapidly absorbed, moves downward to the water table, and then moves laterally to discharge into the ocean, sounds, and inlets. Surface runoff, if any, drains into the tidal marshes that border the sounds.

The USGS in cooperation with the Cape Hatteras National Seashore conducted several localized studies of the groundwater supplies on the Outer Banks. Brown (1960), Kimrey (1960, 1961), Harris and Wilder (1964), Lloyd and Wilder (1968), Wyrick and Dean (1968), and Lloyd and Dean (1968) investigated specific locations and noted that many areas on the Outer Banks can supply adequate potable water for pumping.

Wyrick and Dean (1968) reported that two galleries, one on Ocracoke Island and the other on Hatteras Island, have been installed to supply potable water for camping areas. The gallery on Hatteras Island (Salvo Campground) is about 125 ft long. It was constructed of 20-ft sections of 2-in. diameter pipe alternating with 5-ft screens and was installed in a gravel-packed ditch. The gallery is located near the sound at a

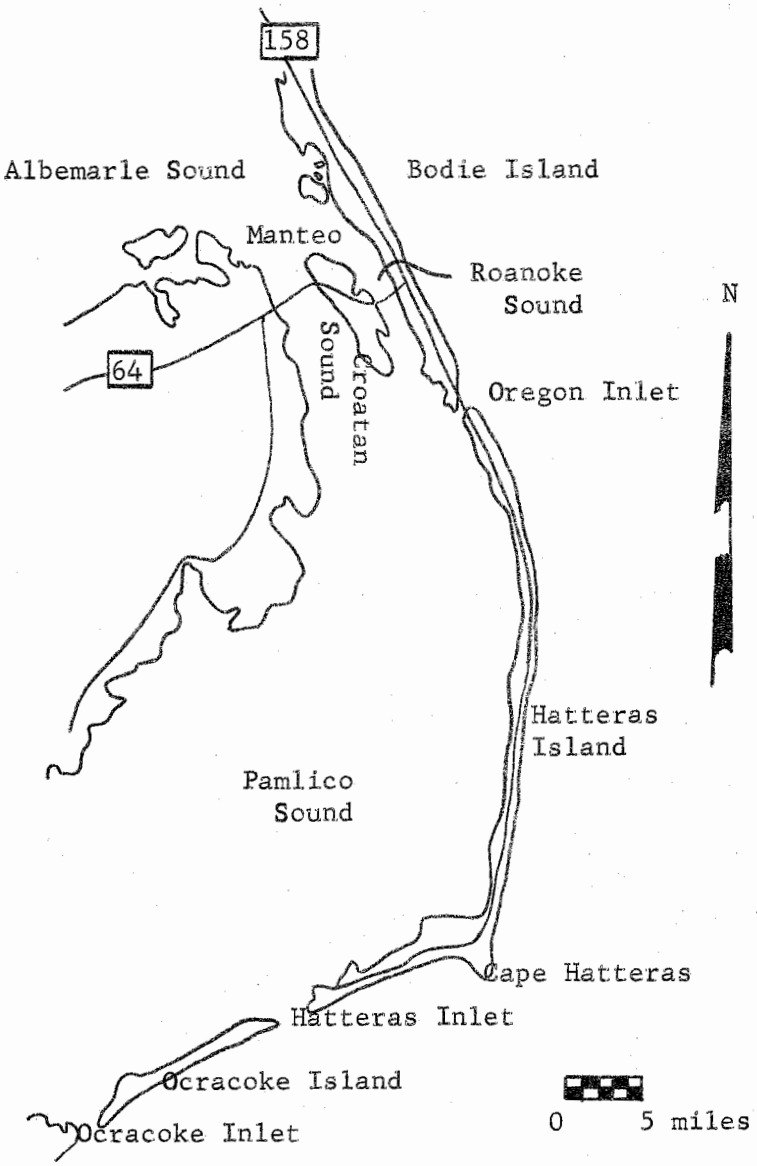

Figure 1. Map of the Outer Banks of North Carolina (after Harris and Wilder, 1964)

depth slightly below mean sea level. Pumping rates greater than 9 gpm resulted in salt water encroachment to the gallery.

The gallery on Ocracoke Island (Parker's Hill) is approximately 220 ft long and 2 in. in diameter. It was constructed of alternating sections of 10-ft lengths of plastic pipe and 5-ft lengths of plastic screen. The pipe was set in the center of a gravel packed ditch approximately 1 ft below mean sea level. The mean water level at the gallery location during 1965 was about 2.5 ft above mean sea level. During pumping tests, the maximum planned pumping rate of 25 gpm was found to lower the water table to the gallery. During the 4 days of pumping, no indication of salt water intrusion was found.

Harris (1967) stated that theoretical values are not valid for the relationship of fresh water head to depth of the interface beneath the barrier islands when there is substantial motion of fresh groundwater and where the sedimentary deposits are heterogeneous or anisotropic. He indicated that fresh water occurs in zones of high hydraulic conductivity whereas salty water occurs in zones of low hydraulic conductivity. At one location on Hatteras Island, he found that the concentration of chlorides in the groundwater varied inversely with hydraulic conductivity of the water bearing zones to a depth of about 140 ft.

A zone of diffusion exists at the interface of salt and fresh water. This zone is formed by the mixing of salt water with fresh water as heads are altered by tides, variation in recharge, and other forces including pumping. Cooper (1964) pointed out that where this zone of diffusion exists, the salt water is not static but rather flows

in a continual cycle from the floor of the sea into the zone of diffusion and back to the sea. This flow of salt water causes some loss of energy of the salt water and thus tends to lessen the amount of salt water that occupies the aquifer. The mechanics of this cyclic flow are such that the water in the zone of diffusion becomes less dense than the sea water and rises along a seaward path. As this occurs, salt water from the sea flows into the soil system to replace that which was removed. Model studies by Cahill (1967) substantiated the cyclic flow theory. Cahill reported that cyclic flow takes place in the denser fluid when fresh water flows seaward over intruding ocean water. He also reported that additional mixing of fresh water and salt water is caused by tidal fluctuations.

Heath[1] indicated that the USGS has now begun generalized groundwater investigations on the Outer Banks. The three representative locations that have been selected for field studies are presented in Table 1.

Table 1. Locations for field studies by USGS

Cross-sectional topography	Location
High elevations with narrow width	Milepost 16.5 on Hatteras Island
Low elevations with narrow width	Milepost 29 on Hatteras Island
Low elevations with wide width	Little Kinnakeet Coast Guard Station (near milepost 32) on Hatteras Island

[1]Heath, R. C. 1969. Personal Communication. District Chief, U. S. Geological Survey, Raleigh, N. C.

At each location the USGS is installing a line of observation wells across the island perpendicular to the beach. Several wells that are screened at different depths are located at each of five points across the island with a vertical pumping well located at the island midpoint. Recording rain gauges are located at mileposts 16.5 and 29. The USGS plans to determine the location of the interface before, during, and after pumping at each of the topographic positions. Predictions of safe pumping rates which will be correlated to island dimensions will then be made for other locations on the Outer Banks. Figure 2 shows the groundwater profile at milepost 29 for two different dates as obtained by Floyd[2]. He indicated that highest tides on the Outer Banks occur in the spring and fall. During these seasons the water table near the ocean rises considerably and may actually be higher than the water table at island midpoint.

Wyrick and Dean (1968) indicated that the water on Ocracoke Island generally contains dissolved minerals, carbon dioxide, and organic acids. These constituents cause the water to be acidic and an effective solvent for iron- and manganese-bearing minerals. When the acidic water comes in contact with shell fragments, it dissolves calcium and magnesium carbonates which cause the water to become more alkaline and to have a higher concentration of hardness. The iron and manganese are then precipitated into the aquifer. The quality of the water depends upon the rate of recharge with mineralization of the water being less during

[2]Floyd, E. O. 1969. Personal Communication. Former Hydraulic Engineer, U. S. Geological Survey, Raleigh, N. C.

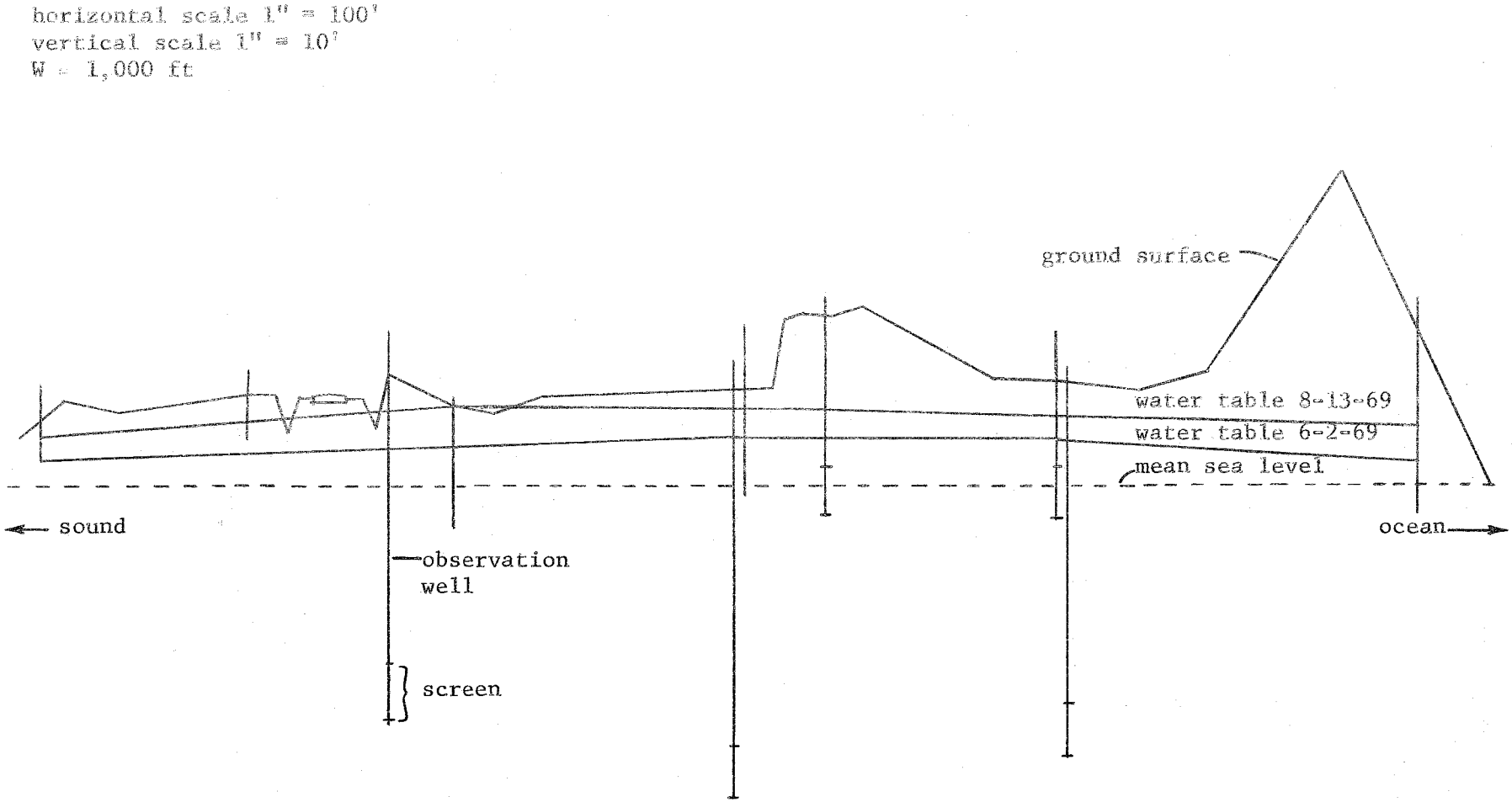

Figure 2. Cross section of Hatteras Island at milepost 29

periods of high precipitation.

Formulations of Interface Location for Long Oceanic Islands

One of the first theoretical analyses of fresh water floating on salt water in porous media was made by Ghyben (Brown, 1925). In his analysis, Ghyben treated the fresh water and salt water as two immiscible, static fluids separated by a sharp interface. The interface, sea level, and water table were assumed to meet at one point; and the surface of seepage was ignored. His results indicated that the elevation of the water table above sea level (z_f) was a constant (α) times the depth to the interface below sea level (z_i). The mathematical expression is

$$z_f = \alpha z_i, \tag{1}$$

where

$$\alpha = (\rho_s - \rho_f)/\rho_f,$$

ρ_f = density of fresh water,

and

ρ_s = density of salt water.

This principle is commonly known as the Ghyben-Herzberg principle. It is based upon the assumption that the constant potential lines in the (two-dimensional) fresh-water regime are vertical. Although the assumption is incorrect, the principle yields results which are close to those derived mathematically if the rate of fresh water discharged is small. Glover (1959), Charmonman (1965), and Verruijt (1968) presented modifications of the principle to account for the flow rate to the sea. In the modifications, the fresh water that flows to the

sea is assumed to be drained away by a horizontal slit as shown in Figure 3.

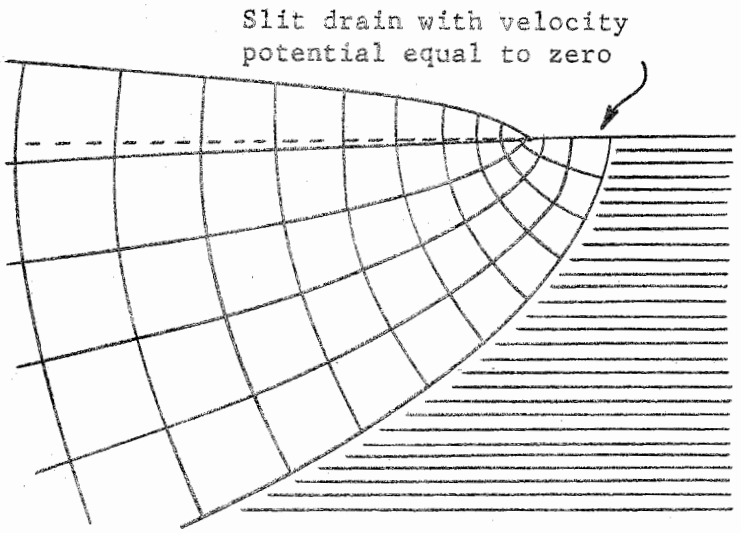

Figure 3. Schematic of flow pattern in a coastal aquifer

By using hodograph solutions, they obtained a relationship for the location of the interface depth. Verruijt (1968) also presented a relationship of the interface depth to free surface height as

$$z_f^2 = \alpha^2 z_i^2 - \left(\frac{1-\alpha}{1+\alpha}\right)\left(\frac{q}{K}\right)^2, \qquad (2)$$

where

K = hydraulic conductivity,

and

q = total discharge of fresh water into the ocean per unit thickness of the aquifer.

When q/K is much smaller than αz_1, the second term on the right hand side of equation 2 may be disregarded and equation 2 is reduced to the Ghyben-Herzberg principle. Verruijt stated that good results should be

obtained by equation 2 if the distance from the sea is large compared to the parameter q/K.

Henry (1964) discussed the validity of the Dupuit assumption for groundwater flow in a long oceanic island. He stated that the influence of the vertical component of velocity may be appreciable when vertical recharge exists. Because the Dupuit assumption neglects any vertical velocities, recharge waters are assumed to enter the aquifer through a continuous distribution of vertical recharge wells from which flow occurs uniformly over the depth from mean sea level to the interface. The resulting equation for the coordinates of the interface is

$$z_1/W = \left\{\frac{R_v}{K_1}\left[\frac{x}{W} - \left(\frac{x}{W}\right)^2\right]\right\}^{1/2}, \qquad (3)$$

where

$K_1 = K\alpha$,

R_v = rate of uniform vertical recharge per unit area,

x = horizontal distance from the shore to the position of z_i,

and

W = width of the island at sea level.

It should be noted that R_v is not necessarily equal to the rainfall intensity, R.

Henry (1964) noted that a more accurate steady state solution would result if two-dimensional potential theory (applying LaPlace's equation) were used. He neglected all flow above the ocean level and assumed a horizontal discharge face in the steady state solution. The boundary velocities were mapped into a hodograph, and subsequent

numerical integration was performed. Figure 4 presents curves showing the interface location for R_v/K_1 = 0.755 and 0.0062 as determined by Henry. Henry indicated that the larger value of R_v/K_1 corresponded to a rate of recharge of 9 in. per day and that the smaller value corresponded to a recharge rate of 27 in. per year for an aquifer having a hydraulic conductivity of K = 40 ft per day and a density difference ratio of α = 1/40. He also indicated that under natural conditions R_v/K_1 would rarely be as large as 0.0062. Henry felt that for many purposes the Dupuit assumption was sufficiently accurate in predicting the interface because Figure 4 shows no difference in the two solutions for R_v/K_1 = 0.0062. The Dupuit assumption causes appreciable error only in situations where the island is wide and the subject of interest is the position of the interface near the shore.

Hantush (1968) presented several time-dependent, potential-theory solutions for the location of the interface of fresh-water lenses. He obtained a solution of the nonlinear differential equation by keeping the distance to the interface constant and by considering the derivatives of the distance to the interface as variables. The resulting linear differential equation was then solved. The distance to the interface that had been kept constant was considered to be a weighted mean of the depth from mean sea level to the interface. This mean was to be obtained during a time period prior to the time that the location of the interface was desired. Hantush presented solutions for three sets of boundary conditions, all of which have both finite and semi-infinite areas of recharge. The three sets included an infinite aquifer, a

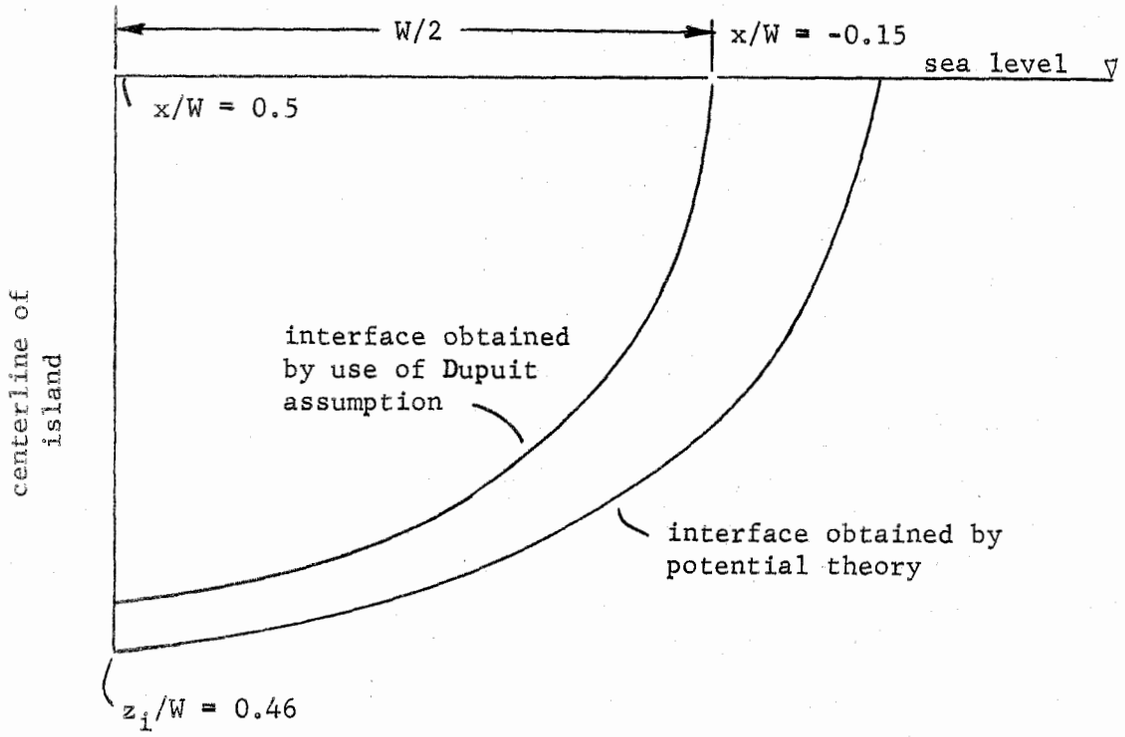

A. Interface for $R_v/K_1 = 0.755$

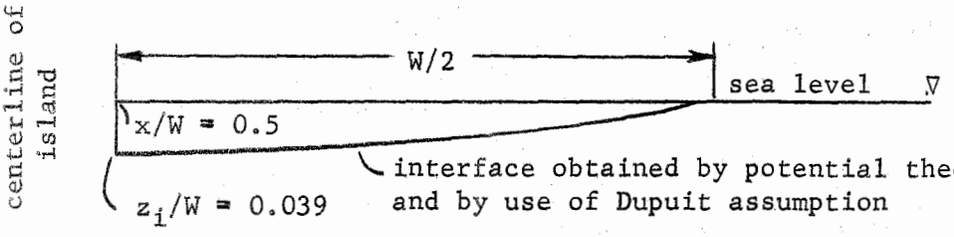

B. Interface for $R_v/K_1 = 0.0062$

Figure 4. Numerical solutions for interfaces in water table aquifers (after Henry, 1964)

semi-infinite aquifer bounded by the ocean on one side with the thickness of the discharge zone assumed to be zero, and a semi-infinite aquifer bounded by an impermeable layer on one side. Hantush also considered horizontal injection wells in each of the above cases. In conclusion, he recommended that his results be checked with a viscous-flow model.

Hele-Shaw Models for Salt Water Intrusion Studies

One of the earliest investigators to use a Hele-Shaw model for salt water intrusion studies was Santing (Todd, 1959). Bear and Dagan (1964) studied the interface in confined aquifers with a Hele-Shaw model having a spacing of 1 mm. Tap water (ρ_f = 1.001 g/cc [grams per cubic centimeter]) and salt water (ρ_s = 1.030 g/cc) were utilized as the viscous fluids. Columbus (1964) also used fresh water and salt water in a Hele-Shaw model to study steady state sea water intrusion into water table aquifers.

De Josselin De Jong (1965) studied confined, steady state flow with water being withdrawn from the aquifer by a gallery. He used resin oil (ρ_f = 0.864 g/cc) and glycerine (ρ_s = 1.071 g/cc) in conjunction with a plate spacing of 2.1 mm and a fluid viscosity of 0.34 cm^2/sec to obtain a hydraulic conductivity of 2.54 cm/sec. Columbus (1966) indicated that Shell Tellus 72 oil (ρ_f = 0.89 g/cc, ν [kinematic viscosity] ≈ 7 stokes) and Pazelus oil satisfy specific weight and viscosity requirements to model sea water intrusion. (The investigator was unable to locate Pazelus oil.) Kashef (1968) studied steady state and transient salt water intrusion into a water table aquifer with a

Hele-Shaw model that had a spacing of 6 mm. Kashef prepared the model fluids by mixing fresh water with a cellulose gum known as carboxymethylcellulose, 7 high premium. Variation in density of the two fluids was obtained by adding salt and sugar to only one of the fluids. Specific gravities of 1.00 and 1.023 were obtained. The model hydraulic conductivity varied from about 60 to about 80 cm/sec.

TWO-DIMENSIONAL FLOW EQUATION FOR A HOMOGENEOUS, ISOTROPIC POROUS MEDIA

The important variables for groundwater flow on a long oceanic island are shown in Figure 5 and are defined when first introduced.

The Darcian velocity potential, φ, at any point is

$$\varphi(x,z,t) = -K\left(z + \frac{p}{\rho_f g}\right), \tag{4}$$

where

g = the acceleration of gravity,

p = groundwater pressure at (x,z,t),

t = time

x = horizontal Cartesian coordinate,

and

z = vertical Cartesian coordinate.

If the flow region is considered symmetrical about the flow line $\overline{ge}$, only one-half the flow region has to be considered in the mathematical analysis. The boundary conditions for region $\overline{gbcefg}$ are as follows.

Along the free surface, $\overline{gb}$, with recharge, $R_v(t)$, the boundary condition (Dagan, 1964) is

$$f\frac{\partial\varphi(x_f,z_f,t)}{\partial t} + [K + R_v(t)]\frac{\partial\varphi(x_f,z_f,t)}{\partial t} = -KR(t), \tag{5}$$

where

f = porosity of the soil

Along the fresh water discharge zone, the boundary condition varies depending upon whether the position is above or below sea level. Positions above sea level within this zone have a variable elevation

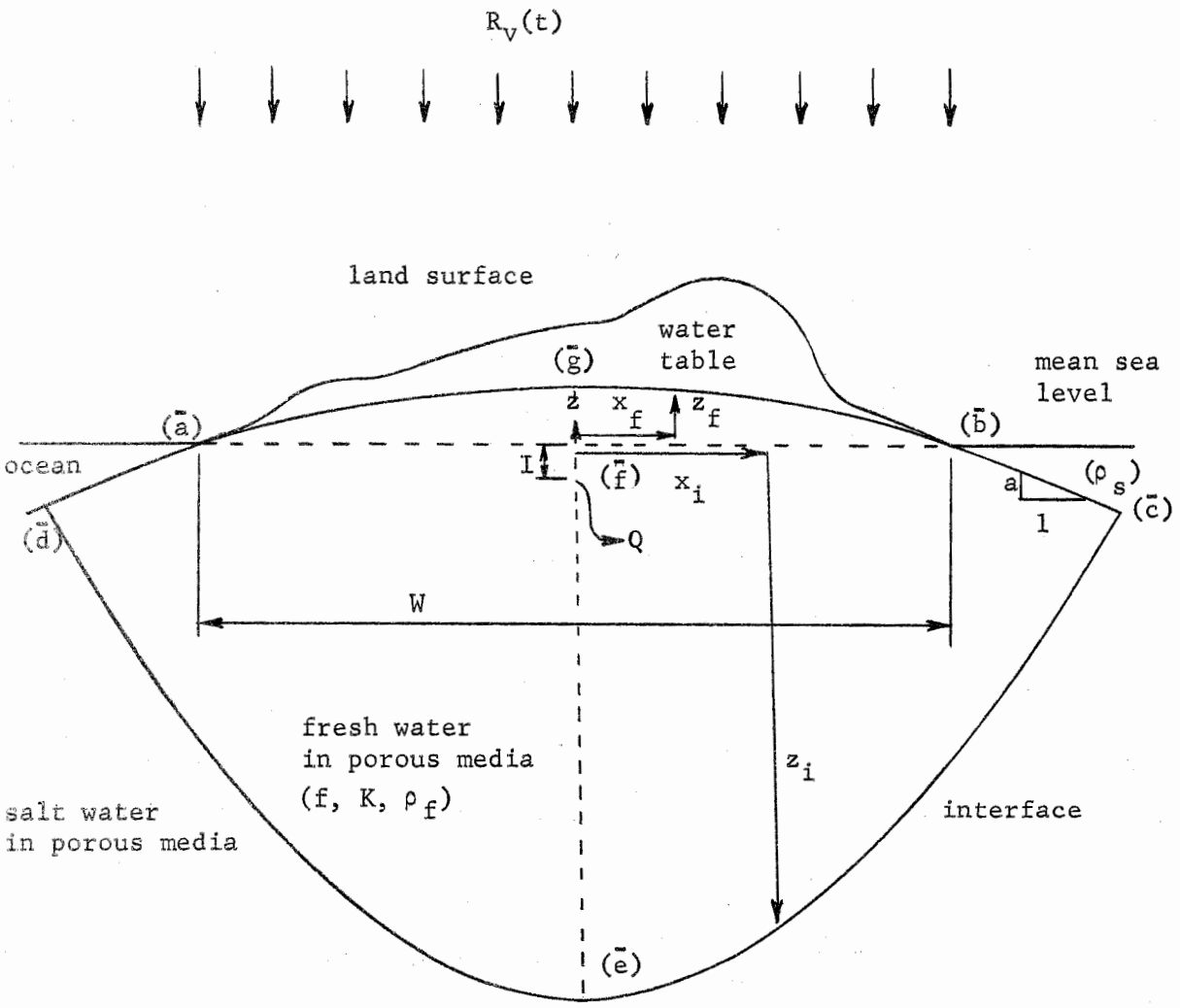

Figure 5. Cross section of a long oceanic island with fresh water lens

potential with a constant groundwater pressure potential (p = 0), while positions below sea level have both variable elevation and groundwater pressure potentials. The boundary conditions for the two regions (along $\overline{bc}$) may be written together as

$$\varphi(x,z,t) = -K\left\{z - [1 - S_0(z)][\frac{\rho_s}{\rho_f}z]\right\} \tag{6}$$

where

$S_0(z)$ = a unit step function defined as

$$S_0(z) = \begin{matrix} 0 & z < 0 \\ 1 & z \geq 0 \end{matrix}.$$

If the salt water in the porous media is considered static, there is no head loss in the salt water zone and the boundary condition for the interface ($\overline{ce}$) may be considered as

$$\varphi(x_i,z_i,t) = -K\alpha z_i. \tag{7}$$

The line of symmetry $\overline{eg}$ is a flow line with the boundary condition,

$$\frac{\partial\varphi}{\partial x}(0,z,t) = 0 \tag{8}$$

except for point $\overline{f}$ which is a sink. The boundary condition at this point is

$$\lim_{r\to 0}(2\pi r V_r) = \lim_{r\to 0}(2\pi r \frac{\partial\varphi}{\partial r}) = Q, \tag{9}$$

where

$r = \sqrt{x^2 + (z - I)^2}$,

I = depth of gallery below mean sea level,

V_r = Darcian velocity in the radial direction,

and Q = pumping rate of fresh water per unit length.

The flow equation may be derived by considering a small cube with sides Δx, Δz, 1 in the saturated fresh-water region. The cube as shown in Figure 6 includes both soil and water.

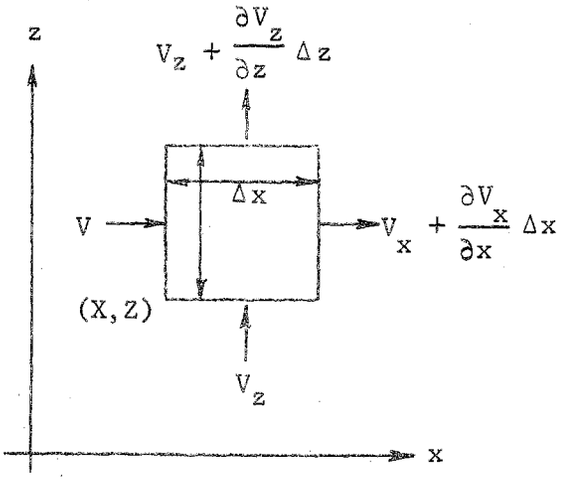

Figure 6. Elemental volume of saturated porous medium

At $x = X$, the velocity in the x direction is V_x; and at $x = X + \Delta x$, the velocity is $V_x + \frac{\partial V_x}{\partial x} \Delta x$. At $z = Z$, the velocity in the z direction is V_z; and at $z = Z + \Delta z$, it is $V_z + \frac{\partial V_z}{\partial z} \Delta z$. The flux into the cube is then $\rho_f[V_x \Delta z + V_z \Delta x]$. The flux out of the cube is

$$\rho_f[(V_z + \frac{\partial V_z}{\partial z} \Delta z)\, \Delta x + (V_x + \frac{\partial V_x}{\partial x} \Delta x)\, \Delta z].$$

The net flux is

$$-\rho_f[\frac{\partial V_x}{\partial x} \Delta x \Delta z + \frac{\partial V_z}{\partial z} \Delta x \Delta z]$$

and is equal to the change in mass of the cube with respect to time. Mathematically, the equality is

$$-\rho_f\left[\frac{\partial V_x}{\partial x}\Delta x\Delta z + \frac{\partial V_z}{\partial z}\Delta x\Delta z\right] = \frac{\partial}{\partial t}(\Delta m) \qquad (10)$$

where

Δm = fluid mass of a cube with sides Δx, 1, Δz.

The space derivatives of the Darcian velocity potential $\varphi(x,z,t)$ give the Darcian velocity. Replacing the velocities of equation 10 with the corresponding potential gradients gives

$$\frac{\partial^2\varphi}{\partial x^2} + \frac{\partial^2\varphi}{\partial z^2} = -\frac{1}{\rho_f \Delta x\Delta z}\frac{\partial}{\partial t}(\Delta m) \qquad (11)$$

A change in the fluid mass with respect to time could result from a change in density of the soil or from a change in density of the water. If the changes in groundwater pressure are small, these changes in mass may be considered as negligible and equation 11 reduces to

$$\frac{\partial^2\varphi}{\partial x^2} + \frac{\partial^2\varphi}{\partial z^2} = 0 \qquad (12)$$

which is the LaPlace equation in two dimensions. Equation 12 along with boundary conditions 5, 6, 7, 8, and 9 represents the mathematical formulation of the physical phenomena. No exact solution to this boundary value problem exists at this time. Thus, numerical techniques or model studies must be used to obtain solutions.

THE ANALOG MODEL STUDY

Formulation of Dimensionless Parameters

The important variables for flow of fresh water in an oceanic island are shown in Figure 5 and are defined where first introduced. Two of these variables, a (slope of discharge face) and f, are dimensionless by definition and are thus two independent dimensionless groupings. When these are omitted, there are 12 remaining variables with a maximum of three (e.g. ρ_f, Q, t) that can be combined in any form without producing a dimensionless grouping. According to Van Driest (1946), the maximum number of independent dimensionless groupings that can be compiled from a set of variables is equal to the number of variables minus the maximum number of variables that can be combined in any form without producing a dimensionless grouping. Thus, there are nine independent groupings from the set of dimensional variables. One set of the nine independent groupings plus a and f is

$$\left(\frac{z_f}{W}, \frac{z_i}{W}\right) = F_1\left(\frac{x_f}{W}, \frac{x_i}{W}, \frac{R}{K}, \frac{Kt}{W}, \frac{\rho_s}{\rho_f}, a, f, \frac{I}{W}, \frac{Q}{KW}\right), \qquad (13)$$

where

W = width of island at mean sea level,

x_f = horizontal coordinate perpendicular to island length and to z_f,

x_i = horizontal coordinate perpendicular to island length and to z_i,

and R = rainfall intensity.

Ligon, Johnson, and Kirkham (1962) stated that the groupings Kt/W (W being any important length term) and f can be combined. The reduced set of groupings is

$$\left(\frac{z_f}{W}, \frac{z_i}{W}\right) = F_2\left(\frac{x_f}{W}, \frac{x_i}{W}, \frac{R}{K}, \frac{Kt}{Wf}, a, \frac{I}{W}, \frac{Q}{KW}, \frac{\rho_s}{\rho_f}\right) \qquad (14)$$

Six of the groupings presented in equation 14 (z_f/W, z_i/W, x_f/W, x_i/W, a, I/W) are composed entirely of geometrical distances and completely describe the geometrical similarity between the model and the prototype (island). The grouping ρ_s/ρ_f describes the importance of the density ratio of salt water to fresh water and puts a severe restriction on the fluids that can be used for modeling. The relative infiltration rate R/K is commonly used because this ratio determines whether ponding of water on the ground surface occurs. Rubin (1966) stated that infiltration will result in ponding if, and only if, R/K exceeds one. The grouping Q/KW describes the pumping rate from a gallery relative to the product of hydraulic conductivity and island width.

If all of the groupings on the right hand side of equation 14 have equal values in model and in prototype, the ratios of free surface and interface locations to island width on the left hand side will also be equal in model and in prototype. The relative locations of the free surface and the interface can be determined from the model, and thus these locations can be predicted for the prototype.

In order to use equation 14 in this study, the density of water in the sound adjacent to the Outer Banks was assumed to be the same as the density of water in the ocean. Also, equation 14 includes the assumptions that the viscosities of the fresh water and the salt water are the same and that the soil system is isotropic and homogeneous. The slope of both beaches (discharge zone) was assumed to be the same for simplicity.

Most porous media found in nature are anisotropic. Thus, a mapping of island coordinates is necessary before an isotropic model can be made similar to two-dimensional groundwater flow in anisotropic porous media. Taylor (1948) presented a method of coordinate transformation that transforms an anisotropic porous media into one that is isotropic. If the axes of anisotropy are horizontal and vertical, the coordinate transformation becomes

$$z^* = \left(\frac{K_x}{K_z}\right)^{1/2} z, \tag{15}$$

where

K_x = hydraulic conductivity in the x direction

and K_z = hydraulic conductivity in the z direction,

and the transformed isotropic hydraulic conductivity becomes

$$K^* = (K_x K_z)^{1/2} \tag{16}$$

where the * represents a coordinate or variable in the transformed isotropic media.

If equation 15 is applied to each dimensionless grouping, the relationships between the values in the model (M) and in the prototype (P) are as follows:

$$\left.\frac{z_f}{W}\right|_M = \left.\frac{z_f^*}{W}\right|_P = \left.\frac{z_f}{W}\left(\frac{K_x}{K_z}\right)^{1/2}\right|_P, \tag{17}$$

$$\left.\frac{z_i}{W}\right|_M = \left.\frac{z_i^*}{W}\right|_P = \left.\frac{z_i}{W}\left(\frac{K_x}{K_z}\right)^{1/2}\right|_P, \tag{18}$$

$$\left.\frac{x_f}{W}\right|_M = \left.\frac{x_f}{W}\right|_P , \tag{19}$$

$$\left.\frac{x_i}{W}\right|_M = \left.\frac{x_i}{W}\right|_P , \tag{20}$$

$$\left.\frac{R}{K}\right|_M = \left.\frac{R}{K^*}\right|_P = \left.\frac{R}{(K_x K_z)^{1/2}}\right|_P , \tag{21}$$

$$\left.\frac{tK}{Wf}\right|_M = \left.\frac{tK^*}{Wf}\right|_P = \left.\frac{t(K_x K_z)^{1/2}}{Wf}\right|_P , \tag{22}$$

$$\left.a\right|_M = \left.a^*\right|_P = \left.a\left(\frac{K_x}{K_z}\right)^{1/2}\right|_P , \tag{23}$$

$$\left.\frac{I}{W}\right|_M = \left.\frac{I^*}{W}\right|_P = \left.\frac{I}{W}\left(\frac{K_x}{K_z}\right)^{1/2}\right|_P , \tag{24}$$

$$\left.\frac{Q}{WK}\right|_M = \left.\frac{Q}{WK^*}\right|_P = \left.\frac{Q}{W(K_x K_z)^{1/2}}\right|_P , \tag{25}$$

and

$$\left.\frac{\rho_s}{\rho_f}\right|_M = \left.\frac{\rho_s}{\rho_f}\right|_P . \tag{26}$$

Model Construction

Figure 7 presents a schematic of the Hele-Shaw model. The two parallel plates were 1/2-in. thick acrylic plastic sheets held apart by washers spaced on 6-in. centers. The washers had a thickness of 0.159 cm $\pm$ 0.002 cm. The parallel plates were held against the washers by No. 10 brass screws inserted through holes drilled in the acrylic plastic. The back plate was mounted to an aluminum frame by 1/4-in. flathead brass screws which were countersunk into the plate. Each plate was 5 ft high and 8 ft long. As shown in Figure 7, a triangular section was cut from each of the top corners of the front plate in order to simulate a sloping beach. Flexible plastic tubing was inserted along the bottom between the parallel plates to serve as a seal.

Acrylic plastic tanks that served as reservoirs were mounted on each end of the parallel plates. Each tank had a vertical slot approximately 1 in. wide that extended the entire height of the tank so that fluid flowing between either tank and the parallel plates was not restricted. A flange was extended on each side of the vertical slots to hold the tanks to the parallel plates. The flanges overlapped the plates for the entire height of the model. The tanks were mounted by inserting screws through the flanges, model plates, and spacers. The joints were sealed by applying Dow Corning Silastic 732 RTV compound.

Each tank had a copper tube outlet located about 2 ft above the bottom of the model. The copper tubing extended to the inside bottom of the tanks so that the tanks could be pumped empty. A gate valve located at each outlet controlled the fluid flow through the outlet.

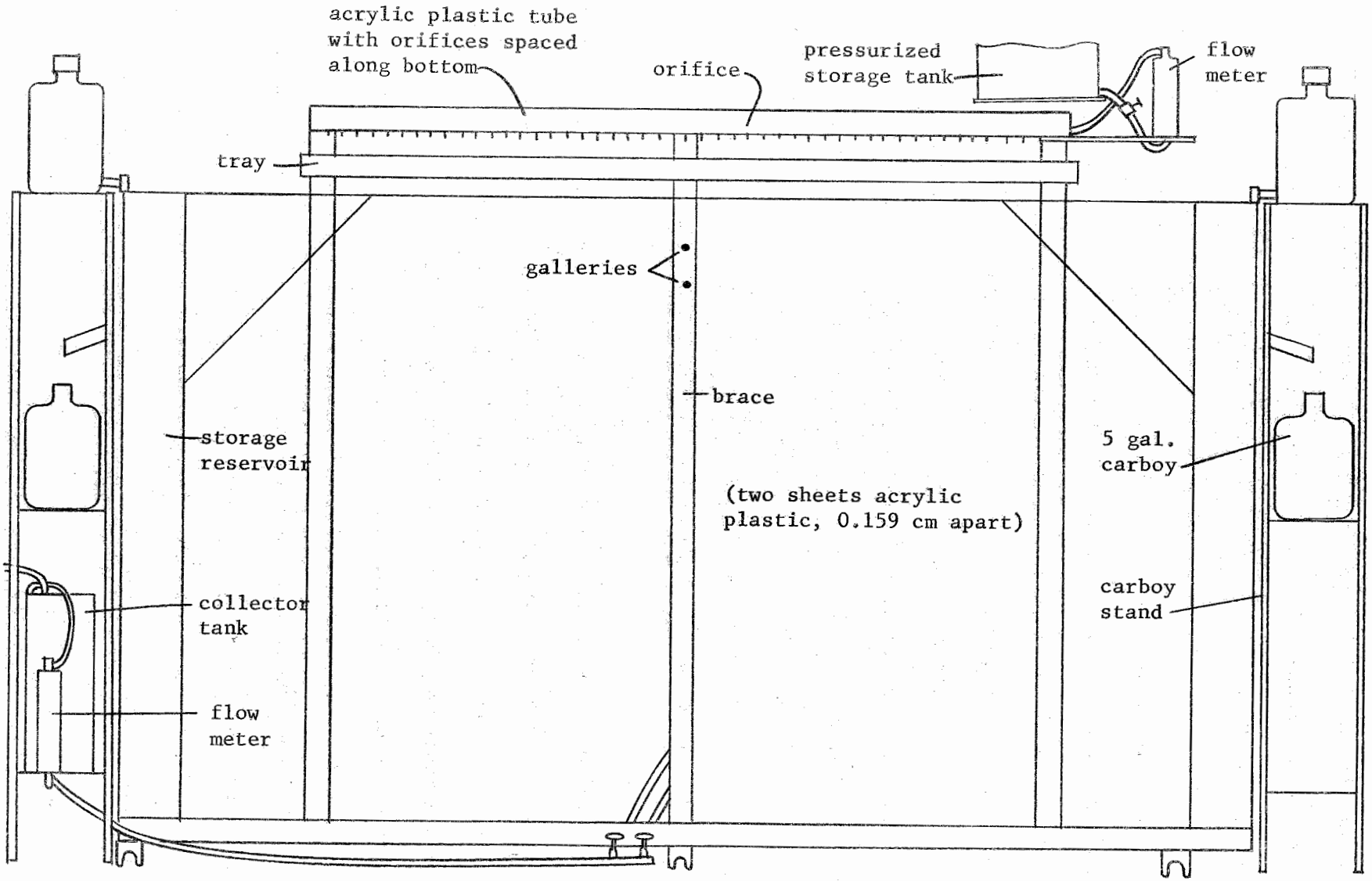

Figure 7. Schematic of Hele-Shaw model

Each tank also had a sliding gate near the top to control the fluid level in the tank. Fluid spilling over each gate was collected in a 5-gal. carboy that was located in a specially constructed rack at each end of the model. Another carboy was located above the first and served to add fluid to the respective reservoir tank.

Fluid was forced through a set of orifices by a pressurized flow system to cause infiltration along the top of the model. The pressure system consisted of a regulated pressure supply connected to a 7-gal. stainless-steel storage tank. The fluid in the storage tank flowed into an acrylic plastic distribution tube after passing through a flow meter and a gate valve. Brass orifices that were installed at 1-in. increments along the bottom of the distribution tube metered the fluid into the model or into a sliding tray that was mounted just below the tube. Fluid was added to the storage tank at intervals by a 1/4-hp gear pump.

The removal of fluid by infiltration galleries was modeled by two different methods. In one method, two holes with radii equal to 0.54 mm were drilled in the back plate of the model. Copper tubing connected the holes to a manifold, then to a flow meter, and finally to a stainless-steel accumulator tank. A vacuum that was controlled by a regulator was applied to the accumulator tank by a laboratory vacuum pump. Different pumping rates were obtained by varying the vacuum. In the second method, holes with radii equal to 0.54 mm were drilled in the front plate of the model which allowed the insertion of a hypodermic needle attached to flexible plastic tubing. The fluid was pumped from

the model by a tubing pump, and its flow rate was measured with a balance and stopwatch. The first method was employed for rates in the range of 2 cc/min and above, while the second method worked better in the range of 0.1 cc/min. A disadvantage of the first method was the requirement to meter a viscous fluid at low flow rates.

Five vertical scales were mounted behind the model and were spaced equally along its length. The scale divisions were alternate black and white sections that were 1 cm in width. The scales were used in conjunction with a cathetometer to obtain the location of the interface and the free surface.

Fluids Used in Model

No existing fluids other than fresh water and salt water could be found to satisfy the requirements for modeling fresh water floating on salt water. These liquids were not used in the model because the low viscosity of water used in conjunction with any practical parallel plate spacing would result in an unacceptably high hydraulic conductivity of the model. Therefore, the two fluids were obtained by adding a viscosity increasing agent to water. The density of one batch was increased by adding salt and sugar. Duplicated values of the density of each fluid were obtained by weighing calibrated pycnometers containing the fluid. The pycnometers held 50 cc of fluid and were weighed to an accuracy of 0.001 gram. Formaldehyde was added to the solutions as a preservative because the viscosity improving agent [carboxymethylcellulose (CMC), 7L] is an organic compound and is subject to decomposition by microorganisms. Red dye was added to the fluid representing

fresh water so that the position of the interface could easily be detected.

High fluid temperatures, stirring, and steam applied directly to the solutions were required for proper mixing because CMC does not dissolve readily in water at room temperature. Final adjustments in the fluid compositions were made by adding water in order to obtain the proper viscosity for the "fresh" or "salt" water solutions. Hercules (1966) noted that the final viscosity of the solution not only depended upon the ingredients, but also depended upon the method of mixing.

Environmental Control

Because the viscosity of the CMC solutions changes with temperature and moisture content, the tests were conducted in an environmentally controlled chamber to minimize these viscosity changes. The temperature was maintained at 22° C $\pm$ 0.5° C, and the relative humidity was maintained at about 50 percent.

Model Calibration

Because variations in the spacing between the parallel plates were thought to be present, calibration of the model was necessary. Charny (Polubarinova-Kochina, 1962) mathematically derived the Dupuit equation which is for steady state flow over an impermeable layer. This equation was employed to calibrate the model. The equation is

$$Q_T = bK(h_1^2 - h_1^2)2L, \qquad (27)$$

where

Q_T = discharge from the model,

b = spacing between the parallel plates,

h_1 and h_2 = heights above the impermeable layer of open bodies of water at the ends of the flow region,

and

L = length of the flow region.

Equation 27 does not incorporate any simplifying assumptions. The hydraulic conductivity of the model as derived by Polubarinova-Kochina (1962) is

$$K = b^2 g/12\nu. \tag{28}$$

Combining equations 27 and 28 and solving for b, yields

$$b = \left(\frac{24LQ_T\nu}{[h_1^2 - h_2^2]g}\right)^{1/3} \tag{29}$$

Because h, the height above the impermeable layer of an open body of water, was not easily controlled, only one set of values of h was employed in the model calibration. The resulting spacing was 0.159 cm, which was the same as the washer thickness.

Procedure

Three of the dimensionless groupings that are presented in equation 14 contain hydraulic conductivity. Each of these three groupings (R/K, Q/KW, and Kt/Wf) was assigned a definite value during each test. Because K was affected by fluid viscosity (as seen in equation 28), another variable in each grouping was altered so that the grouping maintained its required value. However, W and f were fixed so that R,

Q, and t were the only variables that could actually be varied in the model study. For example, consider the modeling of a constant time of infiltration on an island. The variables K, W, and f for the island have fixed values determined by island characteristics. The time interval t fixed the value of Kt/Wf. In the model study W and f were constant, and the hydraulic conductivity K varied with the fluid viscosity. Therefore, the time t of the model varied depending upon K of the model.

The range of values that each dimensionless grouping was assigned was determined by the most prevalent conditions on the Outer Banks or by the desire to create the most critical conditions possible.

The relative infiltration rate R/K was set equal to or less than unity. This upper limit was chosen because, typically, the value of K in sands is 25 in./hr and the infiltration from natural recharge is not likely to be that high. Also, values of $R/K > 1$ produce ponding which was not desired in this study.

The relative time for all occurrences is contained in the dimensionless term Kt/Wf. The relative time during which "fresh water" was being added along the top of the model was denoted by $Kt/Wf = c$. From the beginning of one "fresh water" addition to another, it was denoted by $Kt/Wf = \gamma$. The values of c and γ were held constant during any test so that the addition of "fresh water" was made in cycles of duration γ. The values of γ were calculated to represent "fresh water" application intervals from periods of 1 wk or less to periods of 1 mo or more, depending upon island characteristics. The relative time of "fresh

water" application c was maintained so that the desired total amount of "fresh water" could be added. One complete "fresh water" application cycle as conducted in the tests can be described mathematically as

$$\frac{R}{K} = \begin{cases} \lambda & 0 < \dfrac{Kt}{Wf} \leq c \quad \text{(application of "fresh water" along the top of the model)} \\ 0 & c < \dfrac{Kt}{Wf} \leq \gamma \quad \text{(no application of "fresh water")} \end{cases}, \qquad (30)$$

with

$$0.25 \leq \gamma \leq 1,$$

$$0.002 \leq c \leq 0.036,$$

and

$$0.5 \leq \gamma \leq 4.$$

A recharge parameter, $R_p = \frac{\lambda c}{\gamma} = (R/K)(t_c/t_\gamma)$ was defined so as to be independent of the application cycle. It is defined as the relative infiltration rate, $\lambda = R/K$, multiplied by the fraction of the time that the "fresh water" was being added, $c/\gamma = t_c/t_\gamma$, where t_c and t_γ are the time periods of rainfall and between rainfalls, respectively. The fraction c/γ was so designated in the model because c was the amount of time the "fresh water" was applied and γ was the time from the beginning of one "fresh water" application to the beginning of another.

Most of the pumping tests were conducted with the gallery located in the center of the cross section at mean sea level (I/W = 0) because this position appeared to be the most practical for field application. Several tests were conducted with the gallery being located below mean sea level (I/W = 5/180, 7/180) at the cross section midpoint.

The model was initially made ready by filling it with "ocean"

solution to the height that had been predesignated as mean sea level. The length W of the model at this elevation was 180 cm. In order to simulate a sloping beach, each end of the model had a slope of 45° as shown in Figure 7. The distance from mean sea level to the bottom of the model was 140 cm, and the minimum distance from the interface to the impermeable layer was 55 cm. Thus, the interface was never close to the impermeable layer, and the flow system was considered infinitely deep.

After the "ocean" solution had reached equilibrium, the "fresh water" solution was pumped into the pressurized "fresh water" application system. The viscosities of the two solutions were then measured with a Brookfield rotational viscometer to determine whether both fluids had essentially the same viscosity. Values of R and t were calculated for the predetermined values of λ, c, and γ and were adjusted to counteract variations in K due to changes in fluid viscosity.

The rainfall intensity R was adjusted to the appropriate value while the "fresh water" solution was being caught in a tray instead of being allowed to enter the model. An appropriate timing chart was set up, and the tests were begun. At the time designated by the timing chart, the sliding tray was pulled from beneath the distribution tube, and the "fresh water" solution was allowed to enter the model. The cyclic addition of the "fresh water" solution was continued until no movement in the interface location could be detected. At that time, the location of the interface was recorded at the cross-sectional end points ($z_{i\ 0}$), at the quarter points ($z_{i\ 1/4}$), and the midpoint ($z_{i\ 1/2}$).

The minimum elevation of the free surface was recorded at the cross-sectional end points ($z_{f\ 0}$), one quarter point ($z_{f\ 1/4}$), and the mid-point ($z_{f\ 1/2}$).

Pumping from one of the galleries was then implemented by one of the two previously discussed pumping methods. Initially, the pumping rate was set at a much lower value than the maximum safe pumping rate. After equilibrium was established and the locations of the interface and free surface were recorded, the pumping rate was increased and the process was repeated. The pumping rate was increased in increments until either of two occurrences took place:

1. The free surface dropped to the top of the gallery, and air was being pulled into the system,

or

2. The interface rose to the gallery, and the "salt water" solution began being pumped into the gallery.

Whenever either condition occurred, the test was ended. New conditions were then established, and a new test was initiated.

RESULTS AND DISCUSSION OF THE MODEL STUDY

Location of the Interface under Natural Conditions

Infiltration rates due to rainfall are not likely to reach the high values of hydraulic conductivity of sandy soils on oceanic islands. They will also vary considerably according to the rainfall intensity. Because the natural conditions of varying rainfall intensities are almost impossible to model, tests were conducted to determine the effects of different infiltration rates on the interface location. The infiltration rates employed during the tests were 1/4 K and 1 K. The recharge parameter, $R_p = \lambda c/\gamma$, and the cycle duration γ were held constant during the runs.

The results as presented in Table 2 show that the location of the

Table 2. Location of interface for varying infiltration rates under conditions of no pumping ($R_p = 0.00200$, $\gamma = 4$)

Infiltration rate	$z_{i\ 0}/W$	$z_{i\ 1/4}/W$	$z_{i\ 1/2}/W$
1/4 K	0.0333	0.128	0.144
1 K	0.0444	0.139	0.156

interface was lower for the infiltration rate 1 K. However, the difference is not statistically significant because the standard deviation for $z_{i\ 1/4}/W$ was $s = 0.006$. Thus, the result is a nonsignificant "t" test. The statistical analysis pertaining to the test is presented in Appendix B.

The relative distance $z_{i\ 1/4}/W$ at the quarter point was used as an indicator of interface location instead of $z_{i\ 1/2}/W$ because $z_{i\ 1/4}/W$ was an average of two values and because $z_{i\ 1/2}$ was hard to determine due to dispersion of the fluids at the midpoint. The dispersion at $z_{i\ 1/2}$ was caused by repeated variation of the interface location at that point.

The investigator observed that the "fresh water" added appeared to act as an impulse addition. Since the time of "fresh water" application was short compared to the cycle time (i.e., $c/\gamma < 0.03$), this conclusion appears valid.

Although the differences in the interface location may be caused by a varying infiltration rate, another possible reason for the observed variation was the necessity of using different flow meters to establish the infiltration rates. Because calibration curves for the flow meters depend upon the viscosity of the fluid, variations in viscosity during the calibration period or during a test could cause an error in the flow rate. Another possible error in procedure was the inability of the operator to accurately meter the much shorter input period associated with the higher infiltration rate.

The intervals between rains also vary under natural conditions. Because every rainfall condition could not feasibly be simulated, the "fresh water" was applied in cycles. The cycle duration was varied so as to determine the effect of the frequency of "fresh-water" application on the interface location. Table 3 presents the results of cycle duration (inverse of rainfall frequency) on the interface location with the

Table 3. Location of the interface for varying cycle duration under conditions of no pumping (R_p = 0.00200, λ = 0.25)

γ	$z_{i\ 0}/W$	$z_{i\ 1/4}/W$	$z_{i\ 1/2}/W$
4	0.0333	0.128	0.144
2	0.0333	0.122	0.144
1	0.0306	0.117	0.133

relative infiltration rate, R/K, and recharge parameter, R_p, being held constant. The location of the interface for the shortest cycle duration (γ = 1) is slightly above the other two interface locations, but the difference in the locations was not determined to be statistically significant. See Appendix B. The results from Tables 2 and 3 indicate that the relative infiltration rate and the frequency of rainfall are not dominant characteristics that influence the location of the interface under conditions of no pumping. Thus, the recharge parameter, R_p, may be used to predict the interface location.

Figure 8 presents the relative location of the interface z_i/W as a function of the recharge parameter, R_p, under conditions of no pumping. Each curve shows the relative location of one point on the interface. The grouping z_i/W is the distance from mean sea level to the interface divided by island width at mean sea level. As expected, the depth of the interface decreased with a decrease in the value of the recharge parameter. The decrease appears to be linear when plotted on logarithmic paper.

The results of Figure 8 may be used for an anisotropic porous

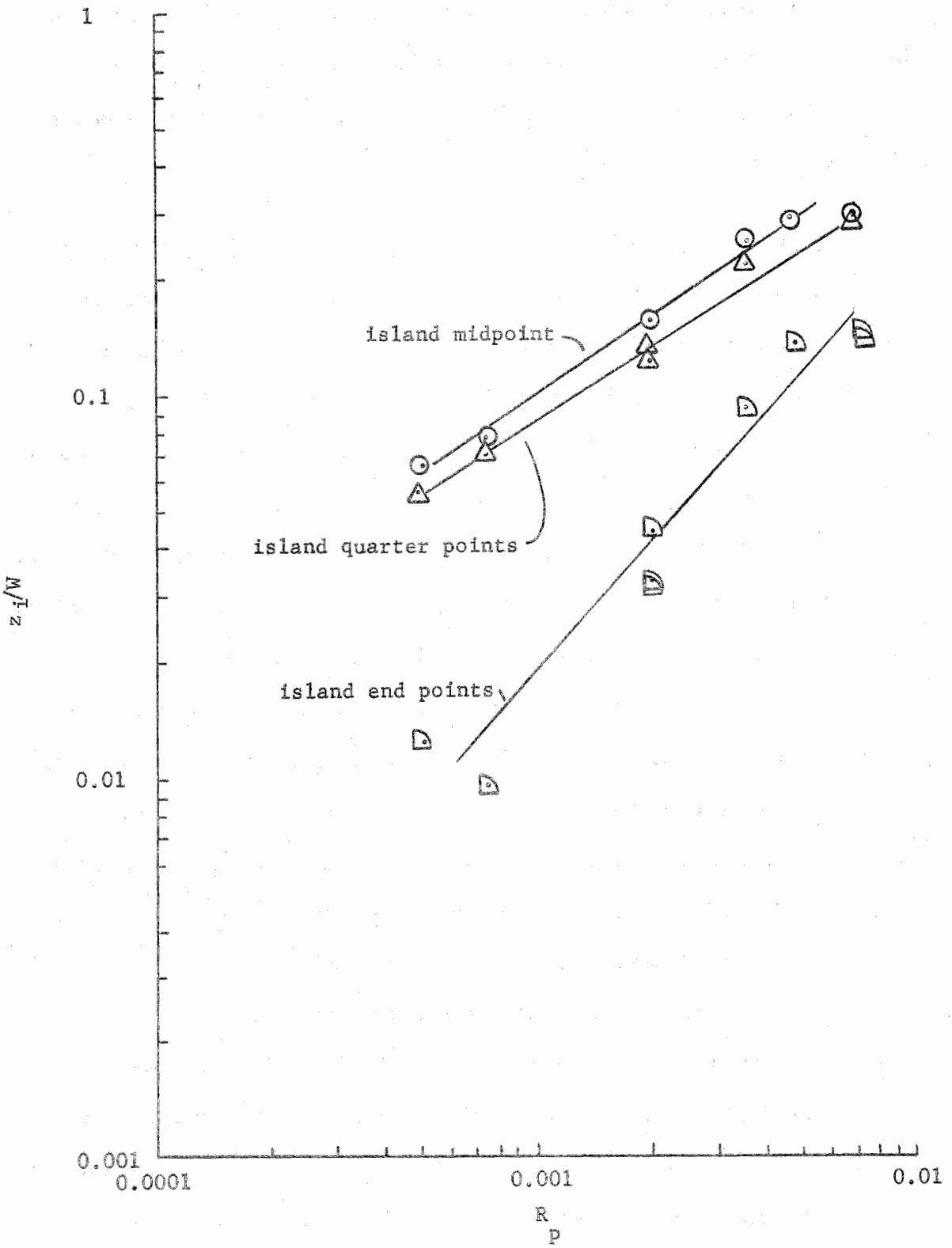

Figure 8. Depth of interface on long oceanic islands (no pumping)

media if an equivalent isotropic hydraulic conductivity is obtained by the use of equation 16. The equivalent hydraulic conductivity is used to determine $R_p = \lambda c/\gamma$, and Figure 8 can then be used to determine $z_i/W\Big|_M$. The relative distance $z_i/W\Big|_P$ for the anisotropic porous media is determined by the use of equation 18.

Effects of Pumping Rate on Locations of Interface and Free Surface

Tests were conducted by pumping at various rates from a gallery located at mean sea level. Figures 9, 10, and 11 show the effects of pumping on the locations of the interface and free surface for several values of the recharge parameter. The ordinate $|z|/W$ which increases upward is a relative distance from mean sea level to the interface or free surface. The abscissa Q/KW which increases to the right is a relative pumping rate. The three upper curves show the effects of pumping on the location of the interface, while the two lower curves show the effects of pumping on the minimum elevation of the free surface. The position of the free surface varied in a cyclic manner for any constant pumping rate because the "fresh water" was applied in cyclic intervals. The minimum elevation occurred just prior to the "fresh-water" addition during each cycle. This elevation was plotted because it represented the most critical position of the free surface.

Figures 9 and 10 show that the distance to the interface was greater at low pumping rates than at no pumping. This paradox was a result of the testing procedure. In most instances in the testing procedure, the infiltration rates were increased between tests so that the interface would move downward more rapidly toward equilibrium.

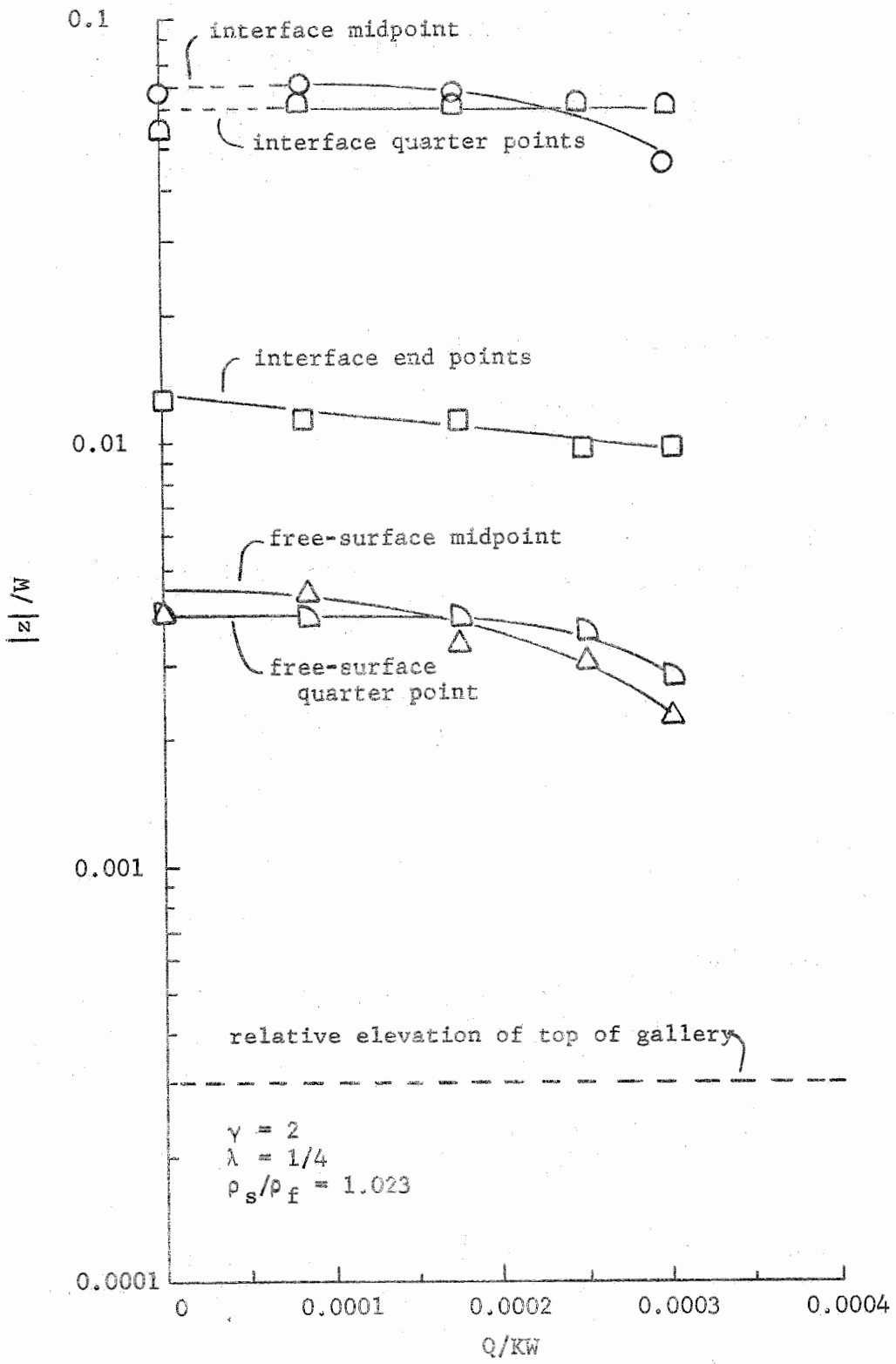

Figure 9. Effect of pumping at mean sea level on interface and free-surface location with $R_p = 0.00050$

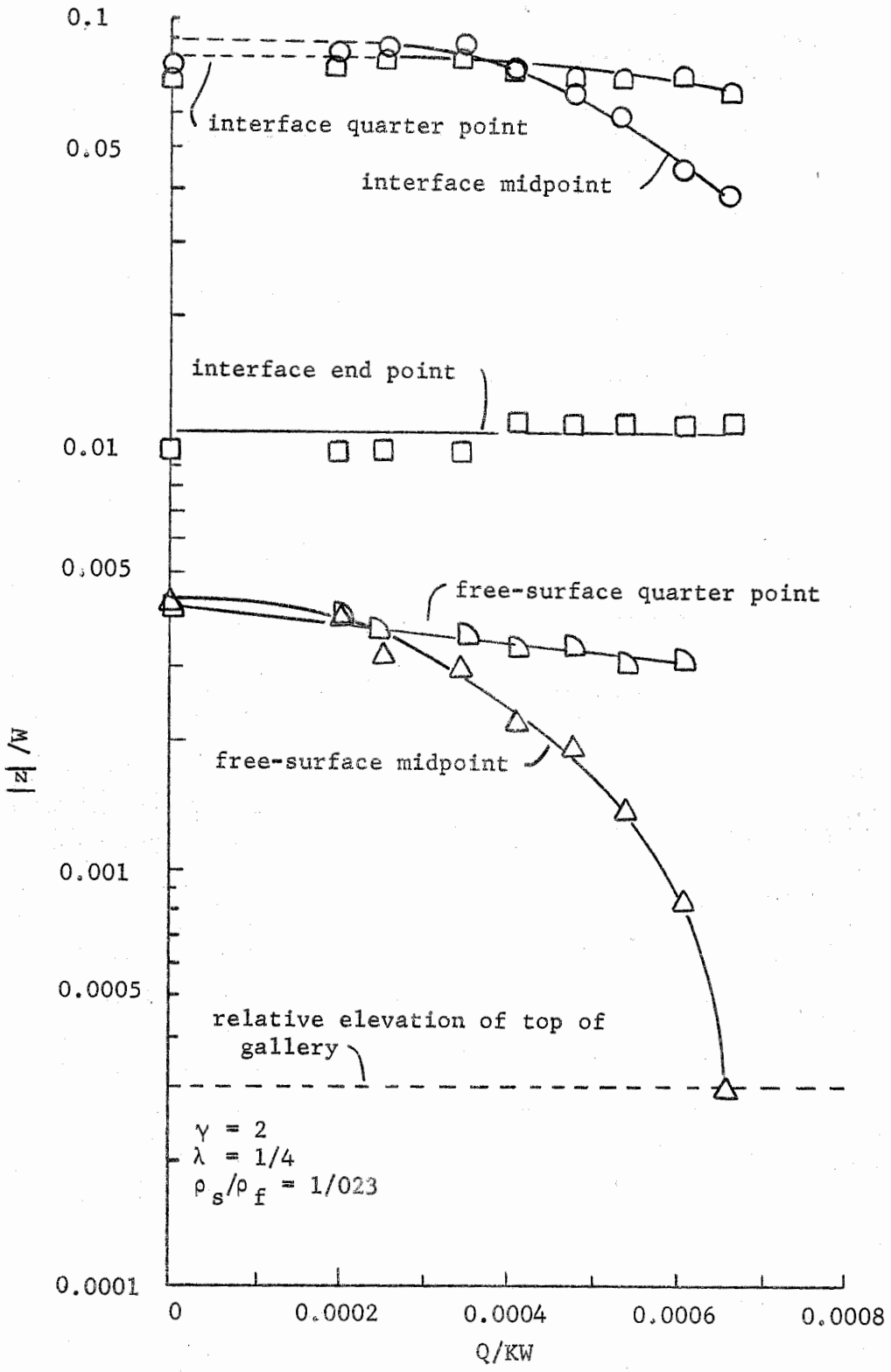

Figure 10. Effect of pumping at mean sea level on interface and free-surface location with $R_p = 0.00075$

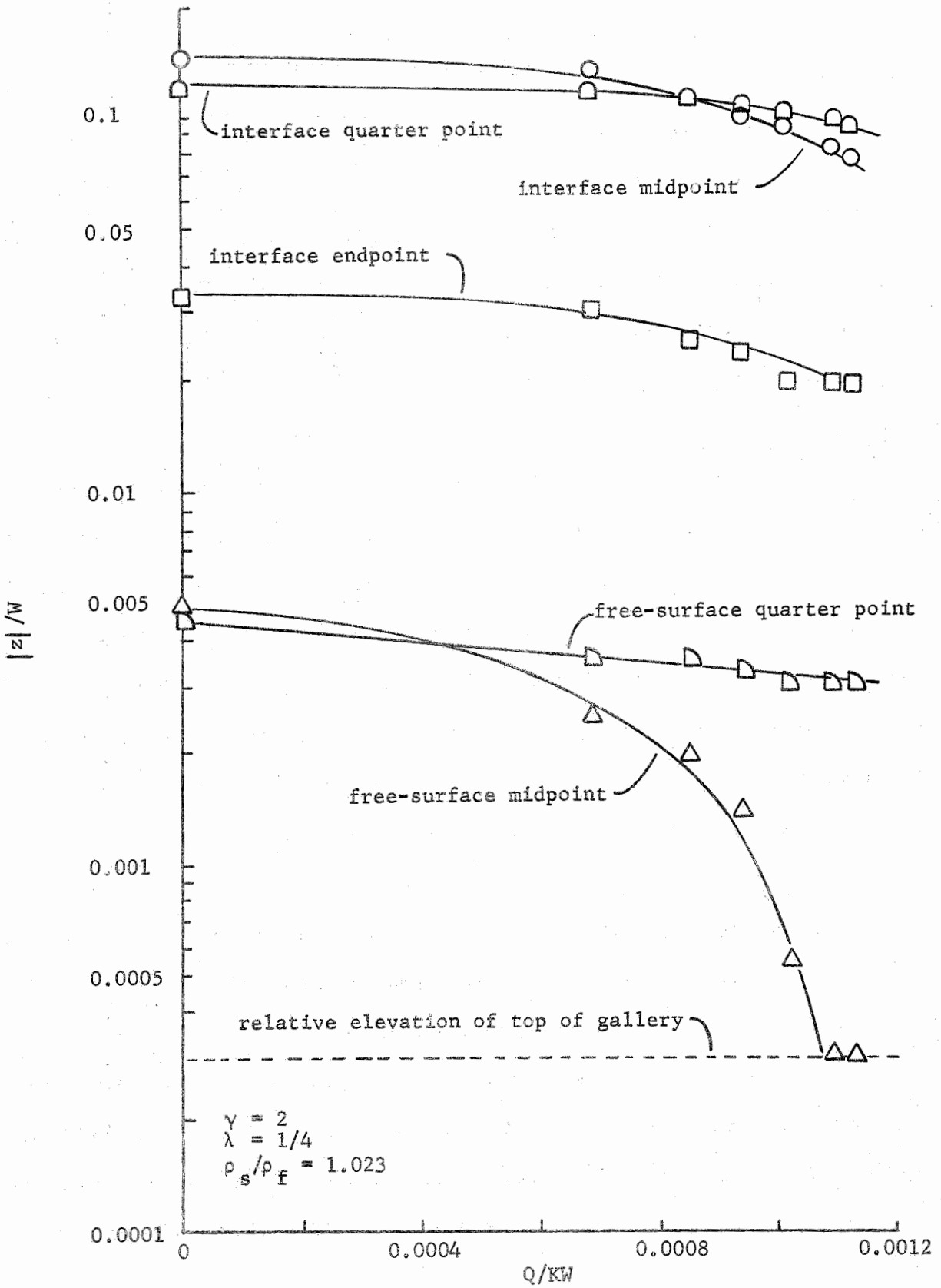

Figure 11. Effect of pumping at mean sea level on interface and free-surface location with $R_p = 0.00200$

As a result, small but observable changes in the interface location were still occurring when pumping was initiated. Because the initial low pumping rate did not affect the interface location, the interface continued to move downward. The curves for the interface location were extended by a dashed line at approximate constant elevations from the maximum relative elevation observed to zero pumping.

The test results presented in Figure 9 for $R_p = 0.00050$ are not complete because the pumping rate was not increased to the maximum rate as described in the subsection entitled Procedure. However, the distance from mean sea level to the interface at the island midpoint was less than at the quarter points for $Q/KW \geq 0.00024$. Such an inversion of the interface location in three-dimensional flow is known as coning. The term will also be applied here even though the flow is two dimensional. The free surface also exhibited a coning effect for $Q/KW \geq 0.00016$ because the distance from mean sea level to the free surface was less at island midpoint than at quarter points. The depth of the interface decreased at all recorded locations as the pumping rate was increased.

Coning of the interface and free surface is also indicated for an increase in the value of the recharge parameter. See Figure 10. However, the interface reached an equilibrium position well below the gallery even for the maximum pumping rate that was obtained when the free surface had dropped to the gallery ($|z|/W = 0.0003$). The location of the interface at the island end points was not affected by pumping.

As shown in Figure 11 with $R_p = 0.00200$, a further increase in the

value of the recharge parameter almost eliminated the coning of salt water even though the free surface was again dropped to near sea level. A cone of depression of the free surface was observed for pumping rates $Q/KW \geq 0.00043$. Pumping of the fresh water caused the interface to move upward at all recorded points.

An additional increase in the value of the recharge parameter was unnecessary because normal conditions do not exceed the value $R_p = 0.00200$. For example, consider the extreme conditions of an infiltration rate of 4 in./wk (high average infiltration rate) with a soil hydraulic conductivity of 10 in./hr (low hydraulic conductivity for sand). These values yield $R_p = 0.00240$ which is only slightly more than the value of R_p in Figure 11. Because critical flows occur during times when the value of the recharge parameter is low, higher values need not be considered. Some results with higher values of the recharge parameter are presented in Appendix B.

Because the elevations of the free surface and the interface at the island midpoint are the most important indicators for determining salt water intrusion, the effect of pumping at mean sea level on these relative elevations has been plotted for various values of the recharge parameter with $\gamma = 2$ and $\lambda = 0.25$. See Figure 12. It should be noted that in all cases the maximum pumping rate is limited by the drawdown of the free surface and not salt water entering the gallery. The expected midpoint locations of the interface can be determined from Figure 12 for known values of the recharge parameter and pumping conditions.

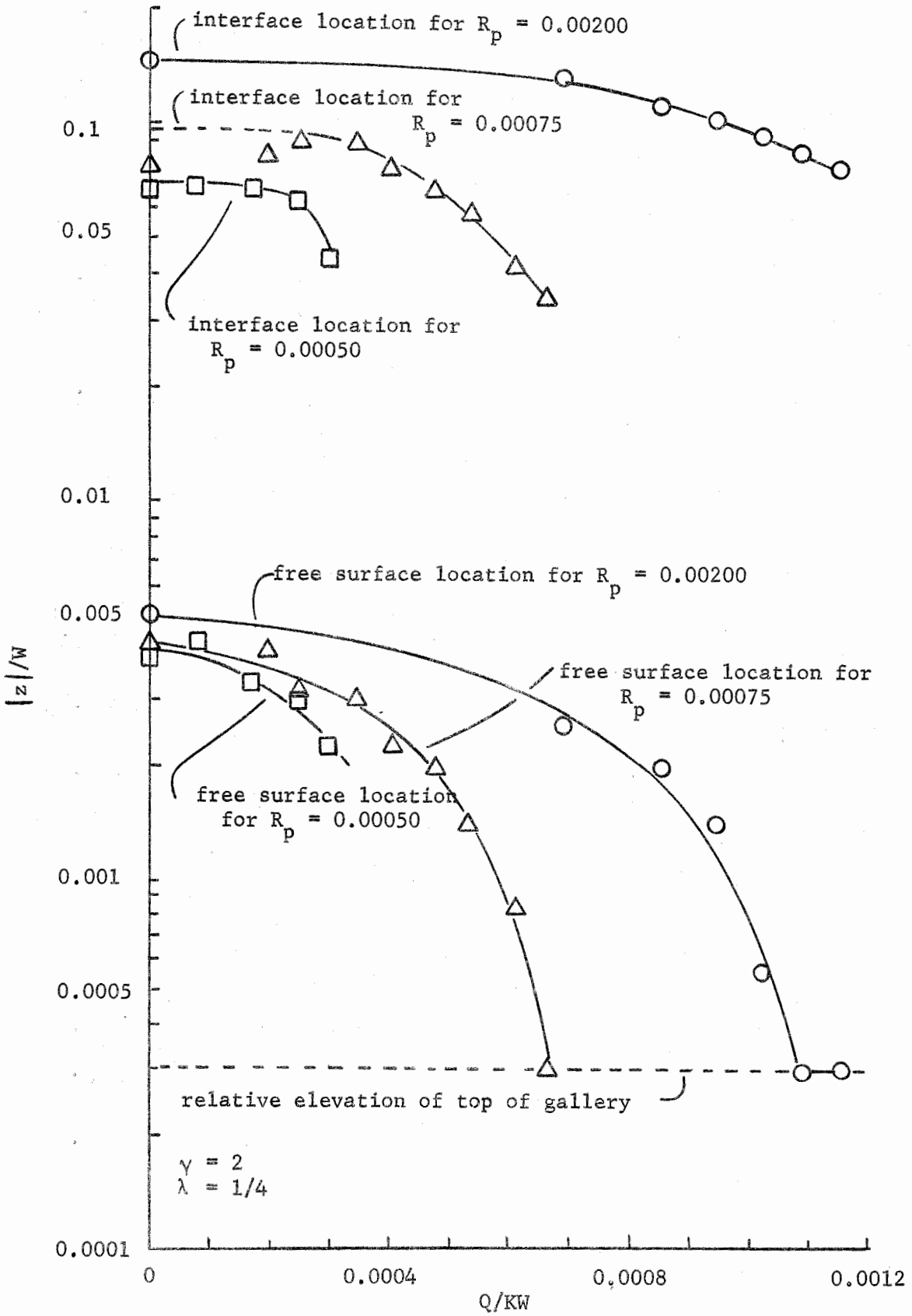

Figure 12. Effect of pumping at mean sea level on midpoint interface and free surface locations for various infiltration rates

Because one of the purposes of this investigation was to determine the amount of fresh water available on a long oceanic island, the exact location of the interface was not of major concern when the maximum pumping rate from a gallery located above mean sea level was limited by the drawdown of the free surface. Therefore, no tests were conducted for the specific purpose of determining whether changes in γ and λ affected the location of the fresh water - salt water interface. However, four experiments were conducted with $R_p = 0.002$ and λ and γ varying. Because the results of these experiments showed no general trends due to variations in λ or γ, and because it was previously shown that variations in infiltration rates and frequencies of rainfall application had no statistically significant effect on the location of the interface under conditions of no pumping, it was assumed that any variations in the location of the interface caused by changes in either λ or γ could be tolerated for the purposes of this study.

It must be clearly understood that changes in any one of the variables, R, K, t_c, or t_p, has to be accompanied by a change in one or more of the others in order to hold R_p constant. Thus, a change in the rainfall rate, R, must be accompanied by a change in either the time period of rainfall, t_c, or the time period between rainfalls, t_p. This causes the total quantity of rainfall to be constant for the given period of time under consideration regardless of the intensity and time distribution of rainfall. The total quantity of rainfall is changed only with changes in the recharge parameter, R_p.

Because K is included in both R_p and Q/KW, the effects of variations in K cannot easily be determined. However, this is not considered to be of major concern because the value of K would ordinarily be held constant for a specific location. The curves in Figure 13 which relate maximum pumping rates to the recharge parameter may be used to predict maximum safe pumping rates. This prediction curve is below the 45° line that represents "fresh water" input equal to removal by pumping. As would be expected, less "fresh water" was removed by pumping than was added by infiltration.

The water use efficiency is defined as the ratio of the pumping rate to the recharge parameter [i.e., $(Q/KW)/R_p$] and was greatest at low infiltration rates. It was approximately 60 percent for $R_p = 0.00050$ even though the maximum flow rate was not obtained, and it decreased to less than 50 percent for $R_p = 0.00700$. Because the results for $R_p \geq 0.00480$ were obtained at a slightly decreased fluid density ratio ($\rho_s/\rho_f = 1.020$), this decreased ratio may have affected the water use efficiency. The efficiency at $R_p = 0.00200$ was slightly above 50 percent. This value can be selected as a conservative value of water use efficiency for design work because higher values of R_p do not normally occur.

The results of Figures 9, 10, 11, and 12 may be used for an anisotropic soil by coordinate transformations previously discussed. The maximum pumping rates presented in Figure 13 are not affected by an anisotropic soil system.

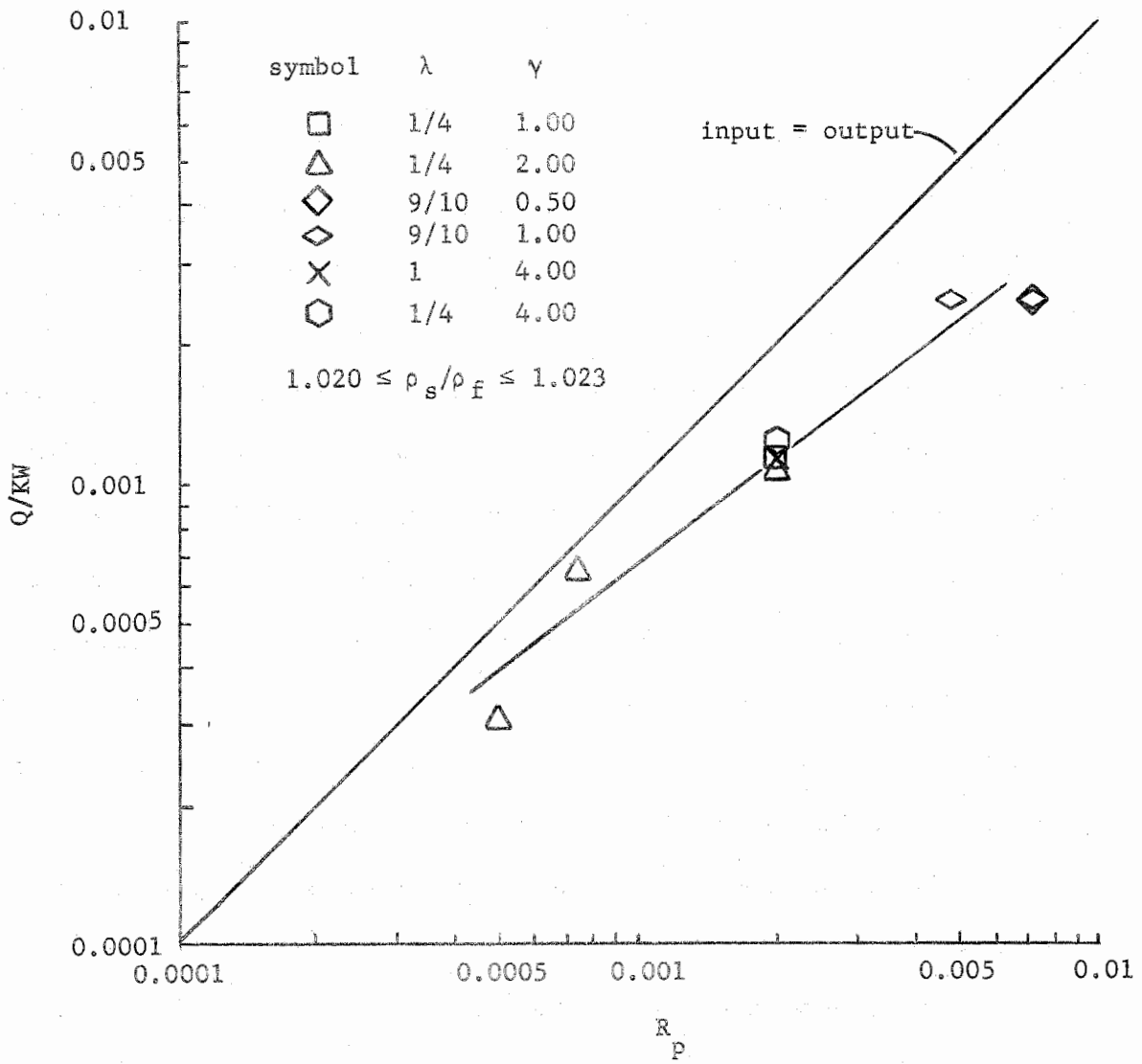

Figure 13. Maximum continuous pumping rate for a gallery located at mean sea level

Pumping from a Gallery Located below Mean Sea Level

In all the preceding tests, the fall of the free surface has been the limiting factor in determining the maximum pumping rate. This result leads to the conclusion that more usable water (higher water use efficiency) may be obtained if the gallery is lowered to a position below mean sea level. Tests were conducted with the gallery at a relative distance I/W = 0.0278 below mean sea level with the recharge parameter R_p = 0.00200. The maximum pumping rate obtained, as shown in Figure 14, was Q/KW = 0.00150 which is a 75-percent water use efficiency $[(Q/KW)/R_p]$. This efficiency is higher than the 50-percent water use efficiency obtained while pumping at mean sea level. All other conditions were held constant for both tests. The increased water use efficiency resulted in the intrusion of salt water to the gallery (coning), and the pumped water became polluted. Figure 14 shows that there is a range from 50- to <75-percent water use efficiency in which increased efficiency is obtained without substantial intrusion. Coning is first indicated at a pumping rate of Q/KW = 0.00110 which gives a water use efficiency of 55 percent. Efficiencies higher than 55 percent were obtained at the expense of much increased pollution of the fresh water lens by salt water.

Figure 14 shows that the minimum free surface elevation at the maximum pumping rate was above sea level. Thus, the gallery was probably located below the pumping position of maximum water use efficiency. However, under actual conditions of varying infiltration and island characteristics, ideal placement of a gallery would be very

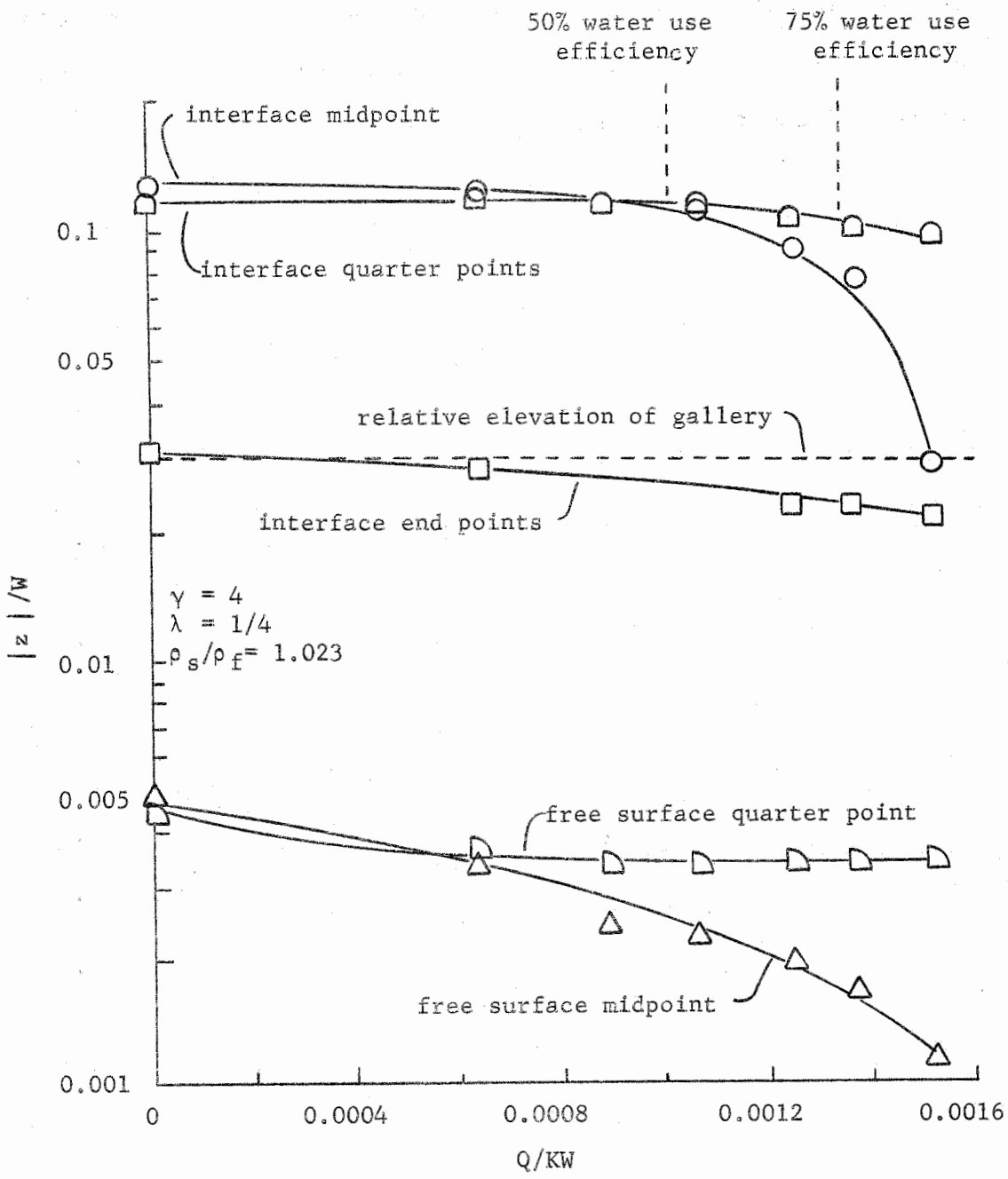

Figure 14. Location of the free surface and the interface for various pumping rates from an infiltration gallery below sea level ($I/W = 0.0278$, $R_p = 0.0020$)

difficult to determine. The results as presented in Figure 14 indicate that the danger of pollution does exist for galleries located below mean sea level and that observation wells would be needed to insure appropriate pumping rates. Indeed, such a safety check would also be advisable for galleries located at mean sea level.

COMPARISONS OF LABORATORY STUDY WITH THEORETICAL AND FIELD STUDIES

Because of the complexity of the system studied in this investigation, no mathematical studies were made. The investigator knows of no mathematical developments that would have been suitable for comparison.

No direct comparisons with field data were made for the following reasons. Firstly, a field study per se was not a part of this investigation. Secondly, an attempt was made to use existing data collected from a horizontal well located on the Outer Banks, specifically the site known as Parker's Hill, but this data was inadequate for comparison purposes. Thirdly, the USGS is presently collecting pumping test data from vertical wells located on the Outer Banks, but no known relationship exists that would allow pumping test data collected from a vertical well to be compared with that from a horizontal well. Although sufficient assumptions could be made to find such a relationship, no reliability could be placed on the final results. However, the results obtained with the Hele-Shaw model in this study are valid because previous drainage investigations that were conducted in our laboratories using this model were not statistically different from mathematical and field results (Rochester and Kriz, 1968; Rochester and Kriz, 1970).

APPLICABILITY OF RESULTS TO LONG OCEANIC ISLANDS

The results of the study are useful to practicing engineers for the following types of problems. Firstly, the location of the interface for varying amounts of rainfall per storm and periods of time between storms under conditions of no pumping allows upper and lower bounds of the interface to be determined so that a more economical field testing procedure can be developed. Secondly, the maximum pumping rate from a horizontal gallery located above mean sea level can be determined for given sets of conditions. Thirdly, the effects of various pumping rates on the location of the interface can be studied for a range of rainfall conditions and island characteristics. Fourthly, the effects of soil anisotropy on the location of the interface can be investigated.

In order to facilitate the use of the results, tabular and/or graphical descriptions of the data collected in the laboratory are presented in this section. Examples of each type of problem described above are also given.

Table 4 presents a relationship between the amount of rainfall per storm, the average length of time between storms, and the location of the fresh water - salt water interface for long oceanic islands under conditions of no pumping. The hydraulic conductivity and the island width must be known before the location of the interface can be determined. Figure 15 presents the data from Table 4 in graphic form in order to facilitate interpolation when necessary.

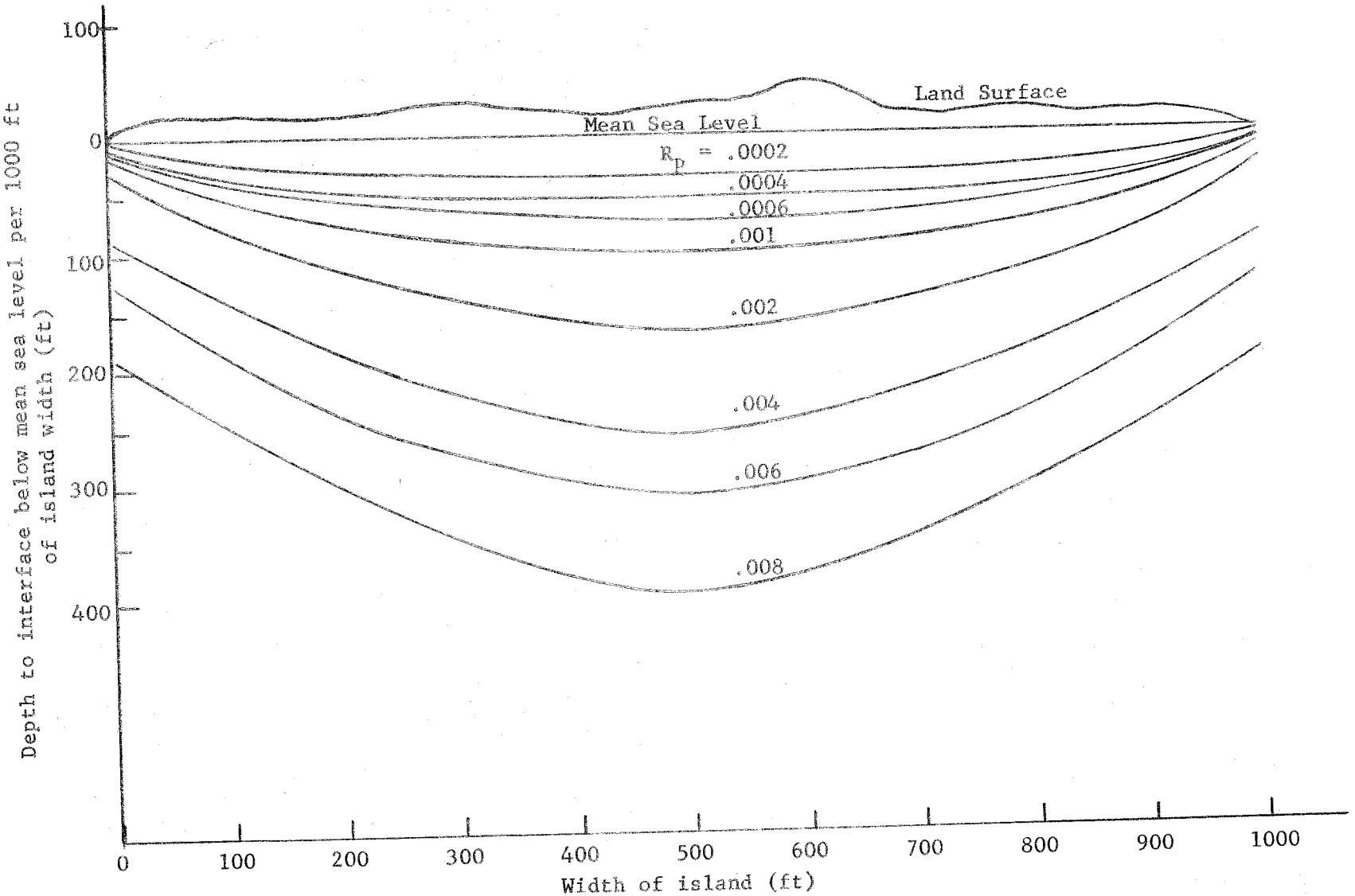

Figure 15. Location of interface for varying amounts of rainfall per storm and periods of time between storms under conditions of no pumping

Table 4. Location of interface for varying amounts of rainfall per storm and periods of time between storms under conditions of no pumping

R_p	Distance from mean sea level to interface per 1000 ft of island width		
	End Points (feet)	Quarter Points (feet)	Midpoint (feet)
.0002	3.5	32	35
.0004	6.9	49	57
.0006	11	62	74
.001	19	88	100
.002	30	130	170
.004	90	205	260
.006	130	260	315
.008	190	305	400

The value of the recharge parameter, $R_p = (R/K)(t_c/t_y)$, in Table 4 can be determined by direct calculation or from Figure 16 for a given set of rainfall conditions and a given hydraulic conductivity. After the value of R_p has been determined, the depth to the interface below mean sea level per 1000 ft of island width can be obtained from Table 4 at the endpoints, quarter points and midpoint of the island. The actual depth to the interface is calculated by multiplying the values by the width of island per 1000 ft.

If the location of the interface and island width are known, Table 4 can be used to determine the value of any one of the following conditions or characteristics provided all the others are known:

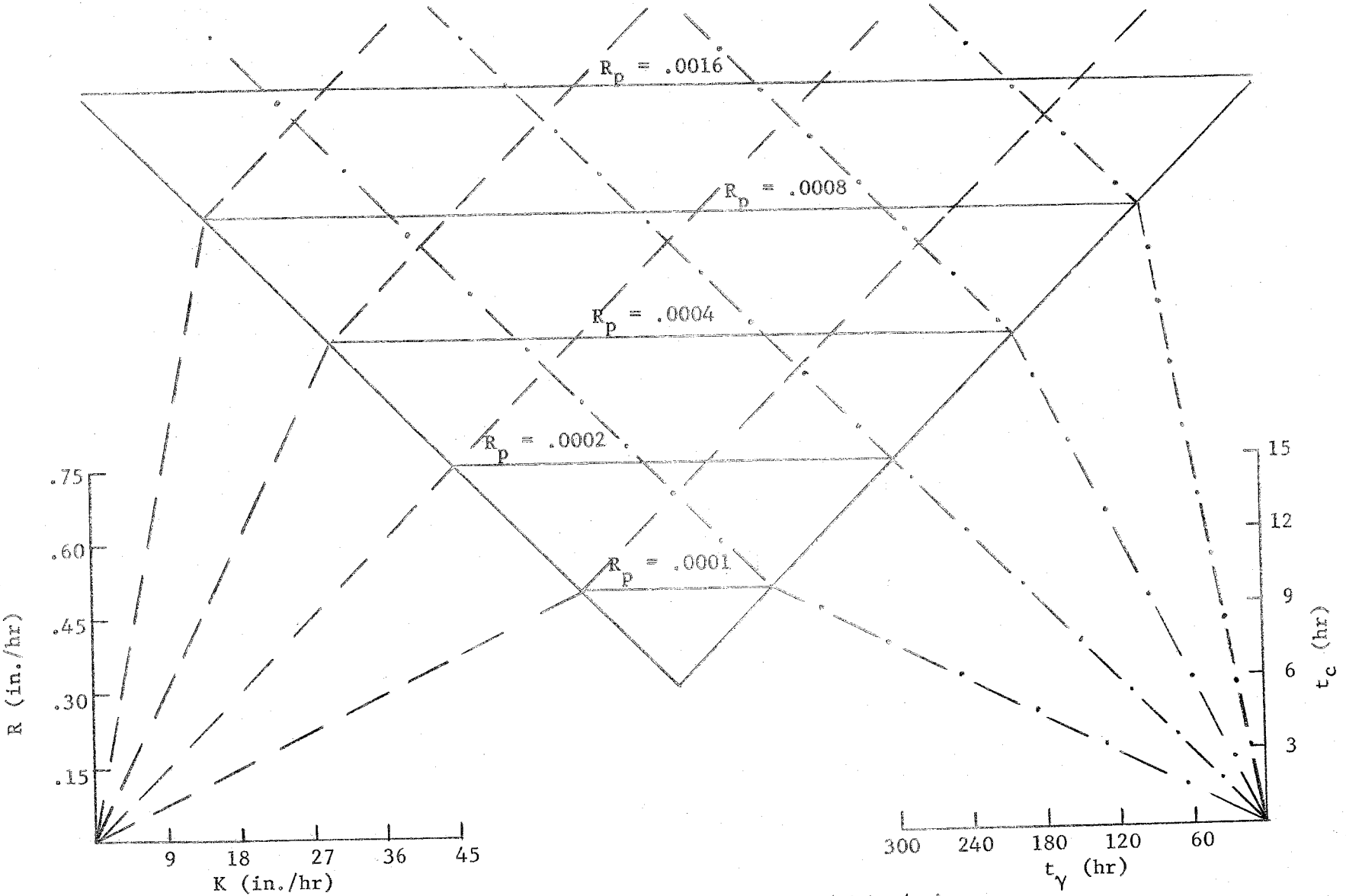

Figure 16. Nomograph for $R_p = (R/K)(t_c/t_\gamma)$

average rainfall intensity, average rainfall duration, average rainfall frequency, or average hydraulic conductivity. The procedure is the reverse of that described above for determining the location of the interface.

Example I

Problem: Determine the location of the interface under conditions of no pumping for a 2000-ft wide island for the following conditions: average rainfall intensity, R, is 0.2 in./hr; average rainfall duration, t_c is 3 hr; average time between rainfalls, t_γ, is 60 hr; and the hydraulic conductivity of the soil, K, is 10 in./hr.

Solution: The value of $R_p = 0.001$ is determined directly by calculation, $R_p = (R/K)(t_c/t_\gamma)$, or from Figure 16. From Table 4 with $R_p = 0.001$, the distance of the midpoint of the interface per 1000 ft of island width below mean sea level is 100 ft. The actual distance is 200 ft([100 ft][2000 ft/100 ft]). Likewise the distances of the interface below mean sea level for the quarter points and end points are 176 ft and 38 ft, respectively.

Example II

Problem: Determine the average hydraulic conductivity for a 1500-foot wide long oceanic island for the following conditions: average rainfall intensity, R, is 0.1 in./hr; average rainfall duration, t_c, is 2 hr; average time between rainfalls, t_γ, is 33.3 hr; and the depth of the interface below mean sea level at the midpoint of the island is 85.5 ft.

Solution: The depth to the interface per 1000 ft of island width is 57 ft([85.5 ft][1500 ft/1000 ft]). From Table 4, R_p = 0.0004. Solving $R_p = (R/K)(t_c/t_\gamma)$ or using Figure 16 to determine the average hydraulic conductivity, K = 15 in./hr.

Table 5 gives tabular values of Figure 13 for the maximum continuous pumping rate for a gallery located at mean sea level at the midpoint of the island for a range of rainfall and island conditions and characteristics. In order to determine this maximum safe pumping rate, the width of the island, rainfall conditions, hydraulic conductivity and length of gallery must be known. Known losses from evapotranspiration should also be subtracted. However, under sandy conditions with little or no vegetation, these losses can be neglected.

The first step in using Table 5 is to determine the recharge parameter, R_p. Once R_p has been determined, the pumping rate, Q, is obtained for the appropriate value of the average hydraulic conductivity, K. The pumping rate is then converted into units of gpm.

Example III

Problem: Determine the maximum safe pumping rate from a 225-ft long horizontal gallery located at mean sea level at the midpoint of a 3000-ft wide island for the following conditions: average rainfall intensity, R, is 0.3 in./hr; average rainfall duration, t_c, is 3 hr; average time between rainfalls, t_γ, is 90 hr; and average hydraulic conductivity, K, is 12 in./hr. An evapotranspiration rate of 0.1 in./day is assumed.

Table 5. Maximum continuous pumping rate for a gallery located at mean sea level

R_p \ K(in./hr)	Pumping Rate (ft^2/hr per 1000 ft of island width)													
	3	6	9	12	15	18	21	24	27	30	33	36	39	42
.0005	.10	.20	.30	.40	.50	.60	.70	.80	.90	1.0	1.1	1.2	1.3	1.4
.0008	.14	.28	.42	.56	.70	.84	.98	1.12	1.26	1.40	1.54	1.68	1.82	1.96
.0010	.17	.34	.51	.68	.85	1.02	1.19	1.36	1.53	1.70	1.87	2.04	2.21	2.38
.0020	.30	.60	.90	1.20	1.50	1.80	2.10	2.40	2.70	3.00	3.30	3.60	3.90	4.20
.0030	.40	.80	1.20	1.60	2.00	2.40	2.80	3.20	3.60	4.00	4.40	4.80	5.20	5.60
.0040	.49	.98	1.47	1.96	2.45	2.94	3.43	3.92	4.41	4.90	5.39	5.88	6.37	6.86
.0050	.58	1.06	1.74	2.32	2.90	3.48	4.06	4.64	5.22	5.80	6.38	6.96	7.54	8.12
.0060	.68	1.36	2.04	2.72	3.40	4.08	4.76	5.44	6.12	6.80	7.48	8.16	8.84	9.52
.0070	.75	1.50	2.25	3.00	3.75	4.50	5.25	6.00	6.75	7.50	8.25	9.00	9.75	10.25
.0080	.83	1.66	2.49	3.32	4.15	4.98	5.81	6.64	7.47	8.30	9.13	9.96	10.79	11.62
.0090	.90	1.80	2.70	3.60	4.50	5.40	6.30	7.20	8.10	9.00	9.90	10.80	11.70	12.60
.010	.95	1.90	2.85	3.80	4.75	5.70	6.65	7.60	8.55	9.50	10.45	11.40	12.35	13.30

Solution: From direct calculation or Figure 16, $R_p = 0.000833$. Interpolating from Table 5, the maximum safe pumping rate without considering any evapotranspiration losses is Q = 0.58 ft^2/hr per 1000 ft of island width. The value of Q is converted into units of gpm as follows:

$$[0.58\ ft^2/hr\ per\ 1000\ ft][3000\ ft\ (island\ width)] = 1.74\ ft^3/hr$$

$$[1.74\ ft^2/hr][225\ ft\ (length\ of\ gallery)][7.5\ gal./ft^3] / [60\ min/hr] = 48.9\ gpm$$

The evapotranspiration loss for the area within the confines of the width of the island and the length of the gallery is as follows:

$$[225\ ft][3000\ ft][0.1\ in/day][ft/12\ in.][7.5\ gal./ft^3] = 42100\ gal./day$$

$$[42100\ gal./day][day/1440\ min] = 29.2\ gpm$$

Thus the maximum safe pumping rate, Q, is [48.9 gpm - 29.2 gpm] = 19.7 gpm.

Table 6 gives a relationship between the pumping rate from a 1000-ft horizontal gallery, the hydraulic conductivity and the parameter, Q/KW. Tables 7 through 9 show the effects of various pumping rates on the location of the interface for a limited range of rainfall and island conditions and characteristics. The tables are based on pumping from a horizontal gallery located at mean sea level at the midpoint of the island. When the rainfall conditions, hydraulic conductivity, and island width are known, the tables can be used to estimate the location of the interface below mean sea level and to study the coning effects of the interface for a given pumping rate. The structure and use of the tables are the same. The differences between the tables are that each is based on a different value of the recharge parameter, R_p.

Table 6. Relationship between the pumping rate from a 1000-ft horizontal gallery, the hydraulic conductivity, and the parameter, Q/KW

K(in./hr) / Q/KW	Pumping Rate (ft^2/hr per 1000 ft of island width)											
	3	6	9	12	15	18	21	24	27	30	33	36
.0000831	.021	.042	.062	.083	.104	.125	.145	.167	.187	.208	.229	.250
.000173	.043	.086	.130	.173	.216	.259	.303	.346	.389	.432	.476	.519
.000200	.050	.100	.150	.200	.250	.300	.350	.400	.450	.500	.550	.600
.000250	.062	.125	.187	.250	.325	.375	.438	.500	.562	.625	.688	.750
.000302	.076	.151	.226	.302	.377	.453	.528	.604	.680	.755	.830	.905
.000347	.087	.174	.260	.347	.434	.521	.608	.694	.780	.868	.955	1.07
.000412	.103	.206	.309	.412	.515	.618	.721	.825	.928	1.03	1.13	1.24
.000481	.120	.240	.361	.481	.601	.722	.842	.963	1.08	1.20	1.32	1.44
.000537	.134	.269	.403	.537	.672	.806	.941	1.07	1.21	1.34	1.48	1.61
.000612	.153	.306	.459	.612	.765	.920	1.07	1.22	1.38	1.53	1.68	1.83
.000666	.167	.333	.500	.666	.834	1.00	1.16	1.33	1.50	1.67	1.83	2.00
.000690	.172	.345	.517	.690	.862	1.03	1.21	1.38	1.55	1.72	1.90	2.07
.000753	.188	.366	.565	.753	.941	1.13	1.32	1.50	1.69	1.88	2.07	2.26
.000792	.198	.396	.595	.792	.990	1.19	1.39	1.58	1.78	1.98	2.18	2.38

(Continued)

(Continued)

Q/KW \ K(in./hr)	3	6	9	12	15	18	21	24	27	30	33	36
.000846	.212	.424	.635	.846	1.06	1.27	1.48	1.69	1.90	2.12	2.33	2.54
.000947	.237	.474	.710	.947	1.18	1.42	1.66	1.89	2.13	2.37	2.60	2.84
.000972	.243	.485	.729	.972	1.21	1.46	1.70	1.94	2.19	2.43	2.67	2.91
.00101	.252	.505	.758	1.01	1.26	1.51	1.77	2.02	2.27	2.52	2.78	3.03
.00124	.310	.620	.930	1.24	1.55	1.86	2.17	2.48	2.79	3.10	3.41	3.62
.00200	.500	1.00	1.50	2.00	2.50	3.00	3.50	4.00	4.50	5.00	5.50	6.00
.00250	.625	1.25	1.87	2.50	3.25	3.75	4.38	5.00	5.62	6.25	6.88	7.50
.00300	.750	1.50	2.25	3.00	3.75	4.50	5.25	6.00	6.75	7.50	8.25	9.00

Table 7. Location of interface for varying values of the parameter Q/KW (R_p = 0.00050)

Q/KW	Distance to interface below mean sea level per 1000 ft of island width		
	Endpoints (ft)	Quarter Points (ft)	Midpoint (ft)
.0000831	11.1	62.5	69.5
.000173	11.1	62.5	66.7
.000250	9.72	61.1	63.9
.000392	9.72	61.1	44.4

Table 8. Location of interface for varying values of the parameter Q/KW (R_p = 0.00075)

Q/KW	Distance to interface below mean sea level per 1000 ft of island width		
	Endpoints (ft)	Quarter Points (ft)	Midpoint (ft)
.000200	9.72	77.8	83.4
.000256	9.72	80.6	88.9
.000347	9.72	80.6	88.9
.000412	11.1	77.8	77.8
.000481	11.1	72.2	66.7
.000537	11.1	72.2	58.4
.000612	11.1	72.2	44.4
.000666	11.1	66.7	38.9

Table 9. Location of interface for varying values of the parameter Q/KW (R_p = 0.0020)

Q/KW	Distance to interface below mean sea level per 1000 ft of island width		
	Endpoints (ft)	Quarter Points (ft)	Midpoint (ft)
.000725	33.5	123.0	139.5
.000950	32.0	121.0	126.0
.00119	29.5	114.9	114.4
.00125	28.0	111.5	110.0

Table 9 is an average of all the tests conducted with R_p = 0.0020. Figures 17 through 19 graphically illustrate the results shown in Tables 7 through 9.

Example III

Problem: Determine whether coning occurs when a 200-ft long horizontal gallery located at mean sea level and 2000-ft wide long oceanic island is pumped at a continuous rate of 30 gpm subject to the following conditions: average rainfall intensity, R, is 0.5 in./hr; average rainfall duration, t_c, is 1.5 hr; average time between rainfalls, t_γ, is 66.7 hr; and the average hydraulic conductivity, K, is 15 in./hr. Losses due to evapotranspiration are considered negligible.

Solution: The first step is to convert the pumping rate from gpm to ft^2/hr per 1000 ft of island width. This is accomplished as follows:

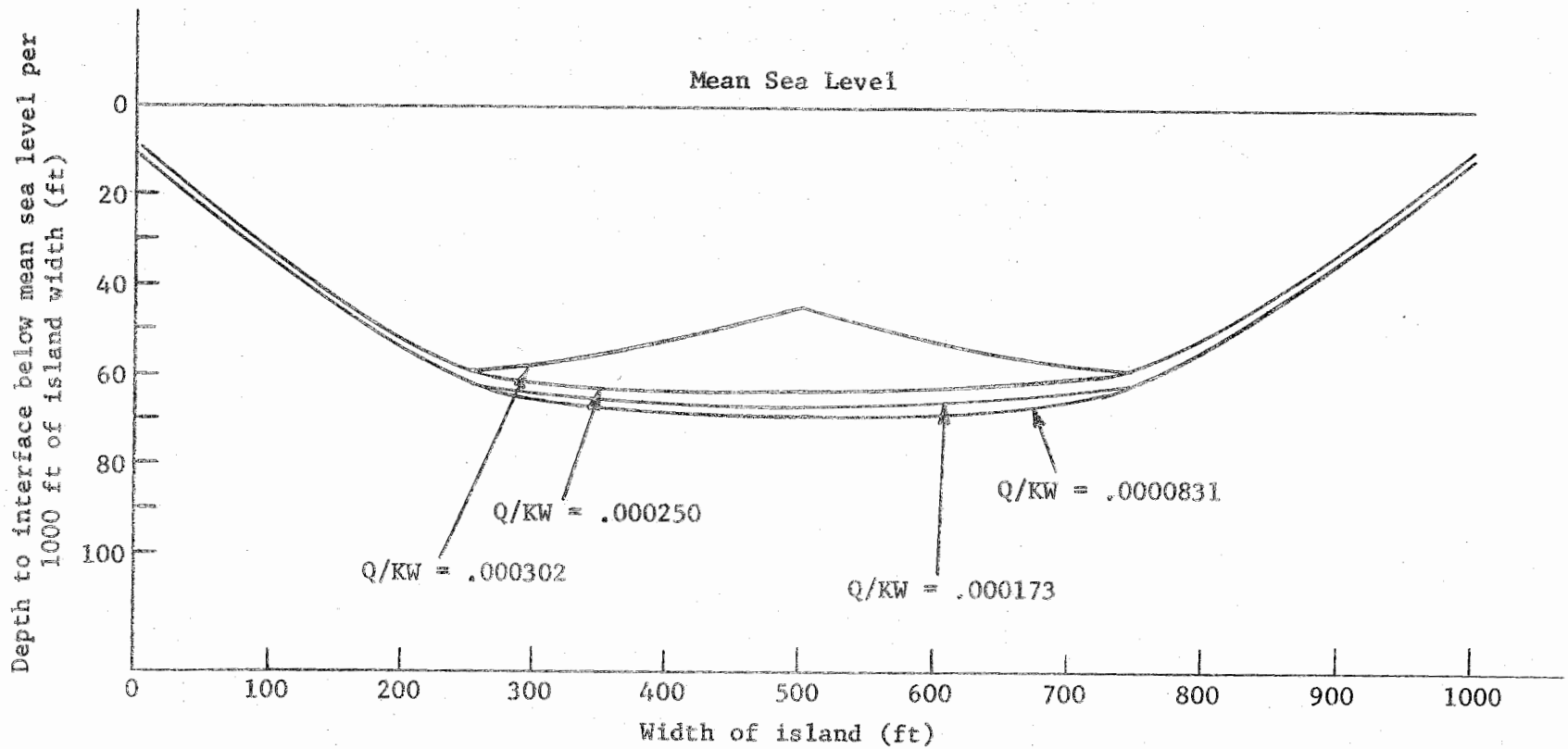

Figure 17. Location of interface for varying values of the parameter Q/KW (R_p = 0.00050)

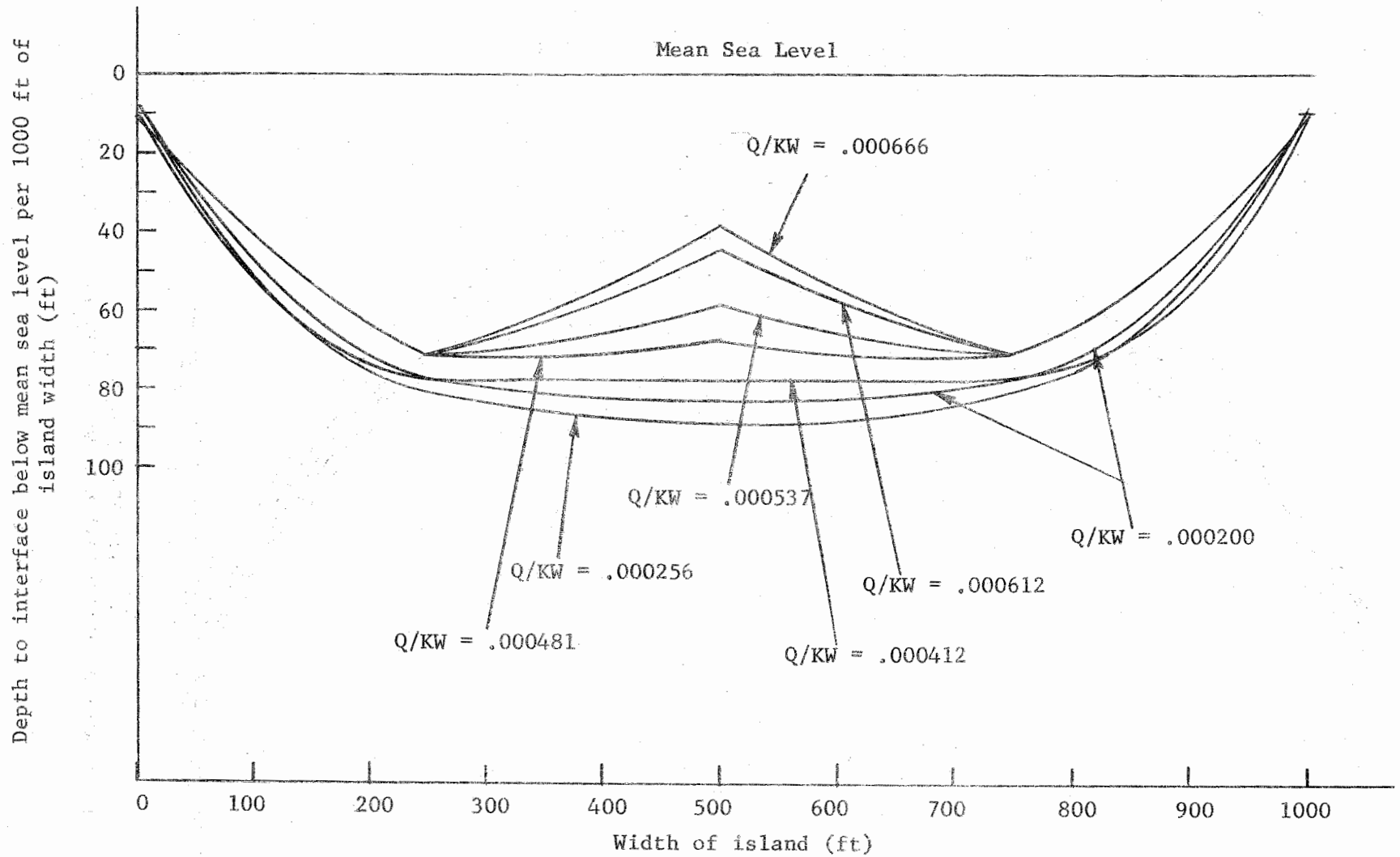

Figure 18. Location of interface for varying values of the parameter Q/KW (R_p = 0.00075)

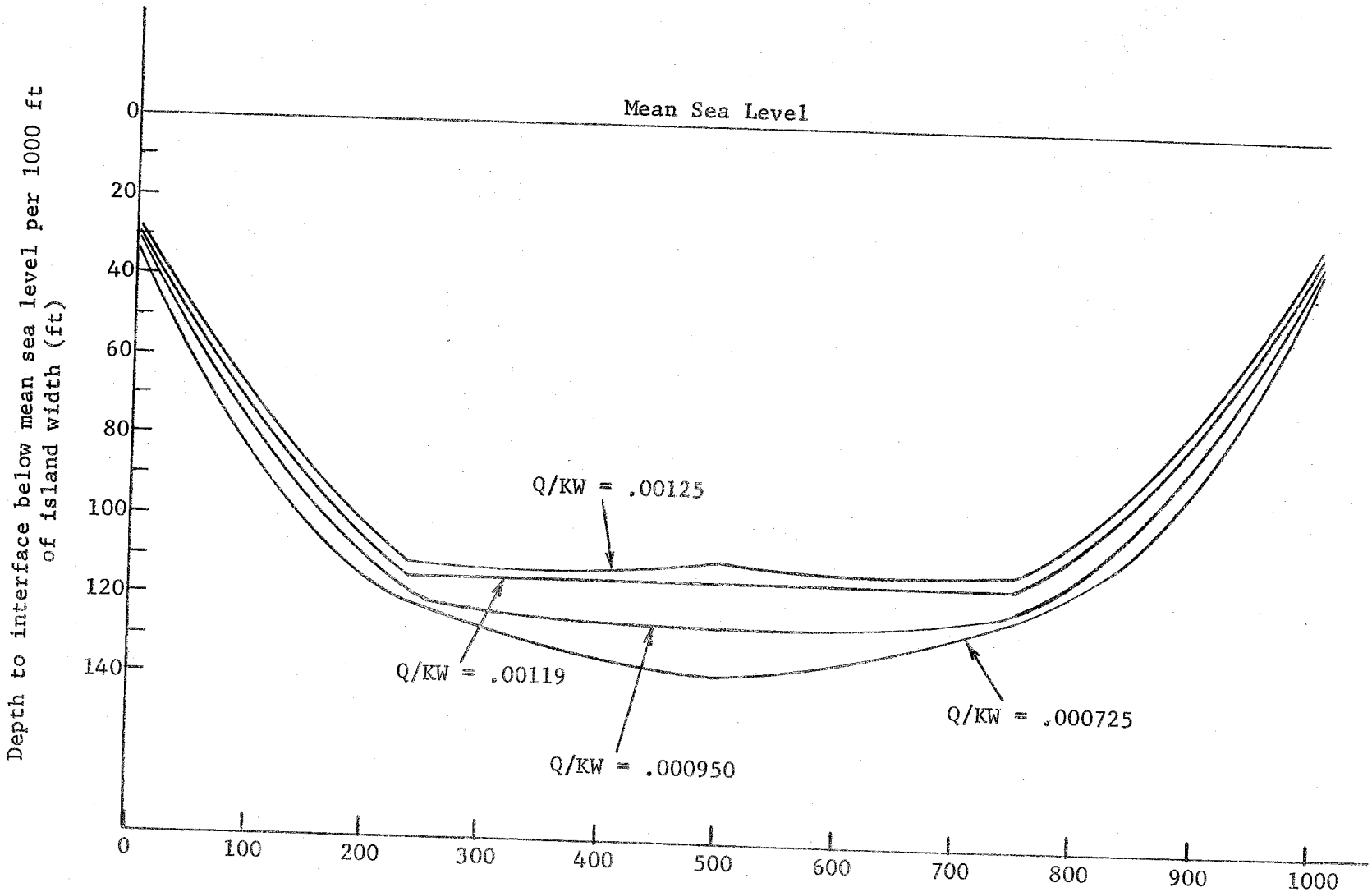

Figure 19. Location of interface for varying values of the parameter Q/KW (R_p = 0.0020)

[30 gpm]/[2000 ft (width of island)/1000 ft] = 15 gpm per 1000 ft.

[15 gpm/1000 ft][60 min/hr]/[7.5 gal./ft^3] = 120 ft^3/hr per 1000 ft.

[(120 ft^3/hr)/1000 ft]/[200 ft (length of gallery)] = 0.60 ft^2/hr per 1000 ft.

Entering Table 6 with Q = 0.60 ft^2/hr per 1000 ft and K = 15 in./hr gives a value of Q/KW = 0.000481.

From direct calculation or Figure 16, the recharge parameter, R_p, is 0.00075. Table 8 or Figure 18 can be used to determine the depth to the interface. For Q/KW = 0.000581, the approximate depths of the interface at the midpoint, quarter points and end points are 66.7, 72.2 and 11.1 ft per 1000 ft of island width, respectively. The approximate depth at the midpoint is 133.4 ft ([66.7 ft/1000 ft][2000 ft(width of island)]. Likewise the approximate depths at the quarter points and end points are 144.4 and 22.2 ft, respectively. Thus, coning does occur for the pumping rate of 30 gpm under the given conditions.

Table 10 is constructed the same as Tables 7 through 9 except that the data is for pumping from a horizontal gallery located below mean sea level at the midpoint of the island. The actual depth of the gallery below mean sea level is expressed as a ratio I/W where I is the depth of the gallery below mean sea level and W is the width of the island. Figure 20 graphically illustrates the data given in Table 10.

The procedure for using Table 10 is identical to that for Tables 7 through 9. Direct comparisons between the effects of pumping from horizontal galleries located at and below mean sea level on the location of the interface can be made for R_p = 0.0020. Because this investigator recommends that the gallery be located at mean sea level, only limited testing was done with the gallery located below mean sea level.

Table 10. Location of interface for varying values of the parameter Q/KW for a gallery located below mean sea level (R_p = 0.0020, I/W = 5/180)

Q/KW	Distance to interface below mean sea level per 1000 ft of island width		
	Endpoints (ft)	Quarter Points (ft)	Midpoint (ft)
0	30.6	117	128
.000638	27.8	117	122
.000894	27.8	111	111
.00107		111	111
.00125	22.2	104	88.9
.00137	22.2	98.7	72.2
.00152	20.8	94.5	27.8

Because many long oceanic islands have anisotropic rather than isotropic conditions, an example is presented to illustrate how the data can be transformed to study anisotropic conditions.

Example IV

Problem: Determine the location of the fresh water - salt water interface under conditions of no pumping on a 2000 ft wide island for the following conditions: hydraulic conductivity in the x direction, K_x, is 25 in./hr; hydraulic conductivity in the y direction, K_y, is 1 in./hr; average rainfall intensity, R, is 0.1 in./hr; average rainfall duration, t_c, is 2 hr; and average time between rainfalls, t_γ, is 3 days.

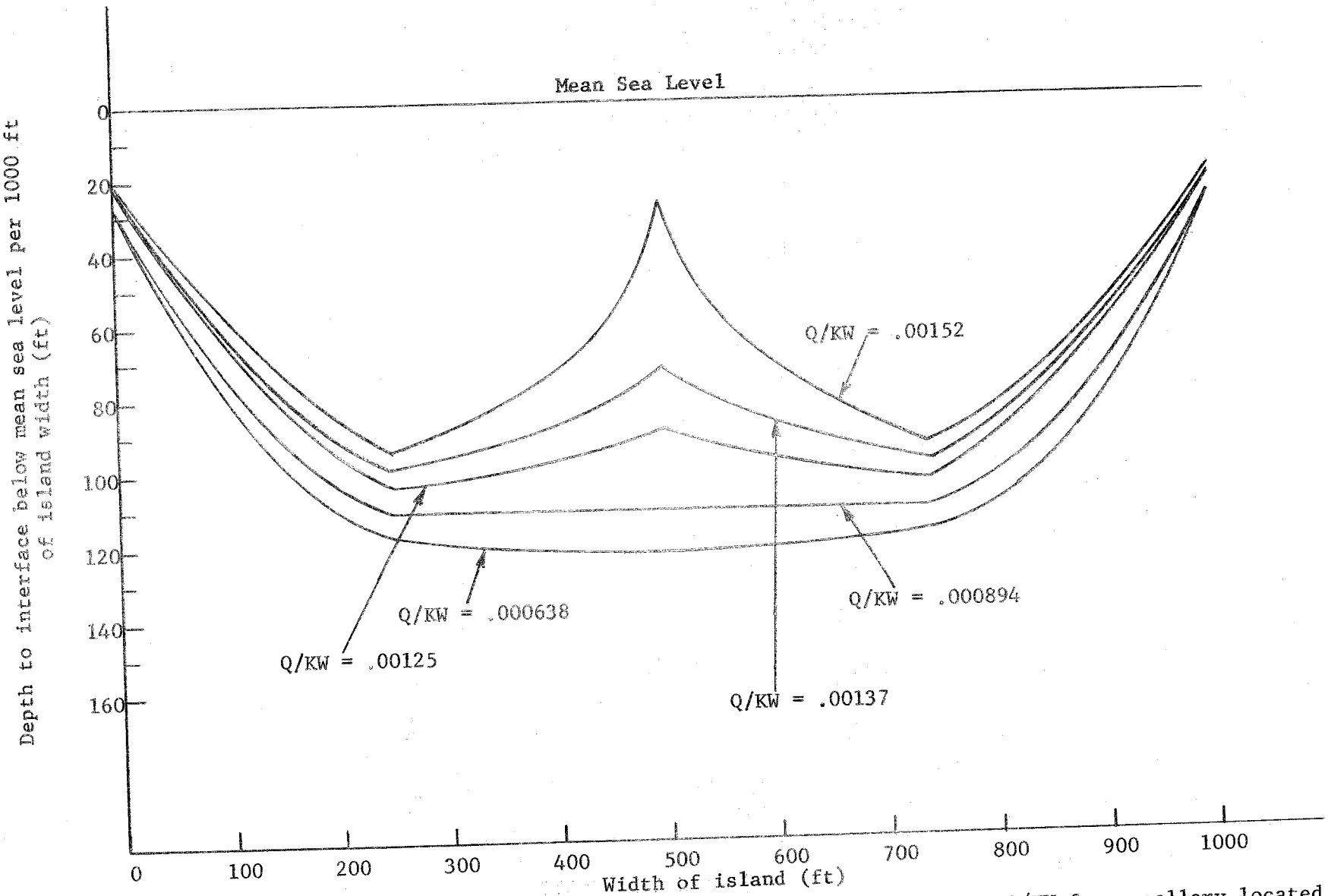

Figure 20. Location of interface for varying values of the parameter Q/KW for a gallery located below mean sea level (R_p = 0.0020, I/W = 5/180)

Solution: The first step is to obtain a value for the transformed hydraulic conductivity, K*, where $K^* = (K_x K_y)^{\frac{1}{2}}$. Thus, $K^* = [(25)(1)]^{\frac{1}{2}} =$ 5 in./hr. It is then necessary to determine what value of R/K in the model corresponds to the R/K* in the field. Because $R/K\Big|_M = R/K^*\Big|_P$, $R/K\Big|_M = (0.1 \text{ in./hr})/(5 \text{ in./hr}) = 1/20$. Using this value, $R_p = 0.0013$ is determined from direct calculation or Figure 16.

From Table 4 or Figure 15 with $R_p = 0.001$, the depths to the interface below mean sea level for the model are 100, 88 and 19 ft per 1000 ft of island width at the midpoint, quarter points and end points, respectively. Because $z_i/W\Big|_M = (z_i/W)(K_x/K_z)^{\frac{1}{2}}\Big|_P$, the depth to the interface per 1000 ft of island width at the midpoint of the island in the prototype is 100/5 = 20. Similarly, values of 17.6 and 3.8 are obtained for the quarter points and end points, respectively.

The actual distance to the interface at the midpoint is $z_i/W\Big|_P$ times the width of the island per 1000 ft or (20 ft)(2000 ft/1000 ft) = 40 ft. Similarly, the depth to the interface is 35.2 and 7.6 ft below mean sea level at the quarter points and end points, respectively.

Maximum safe pumping rates for anisotropic conditions can also be determined by using equations 15 - 26 and following the examples previously given.

LIST OF REFERENCES

Bear, J., and G. Dagan. 1964. Moving interface in coastal aquifers. J. Hydraul. Div. Amer. Soc. Civil Eng. 90:193-216.

Brown, J. S. 1925. Study of coastal ground water with special reference to Connecticut. Water Supply Paper 537. U. S. Geol. Surv., Washington, D. C.

Brown, P. M. 1960. Ground-water supply of Cape Hatteras National Seashore Recreational Area, Rep. Invest. 1. N. C. Dep. Water Resour., Div. Ground Water, Raleigh, N. C.

Cahill, J. M. 1967. Hydraulic sand-model study of the cyclic flow of salt water in a coastal aquifer. Geol. Surv. Res., Chapter B, Prof. Paper 575-B. U. S. Geol. Surv., Washington, D. C.

Charmonman, S. 1965. A solution of the pattern of fresh-water flow in an unconfined coastal aquifer. J. Geophys. Res. 70(12):2813-2819.

Columbus, N. 1965. Viscous model study of sea water intrusion in water table aquifers. Water Resour. Res. 1(2):313-323.

Columbus, N. 1966. The design and construction of Hele-Shaw models. Groundwater 6(2):16-22.

Cooper, H. H., Jr. 1964. A hypothesis concerning the dynamic balance of fresh water and salt water in a coastal aquifer, sea water in coastal aquifers. Water Supply Paper 1613C. U. S. Geol. Surv., Washington, D. C.

Dagan, G. 1964. Linearized solution of unsteady deep flow toward an array of horizontal drains. J. Geophys. Res. 69(16):3361-3381.

De Josselin De Jong, G. 1964. A many-valued hodograph in an interface problem. Water Resour. Res. 1(4):543-555.

Glover, R. E. 1959. The pattern of fresh-water flow in a coastal aquifer. J. Geophys. Res. 64(4):457-459.

Hantush, M. S. 1968. Unsteady movement of fresh water in thick unconfined saline aquifers. Bull. Intern. Ass. Sci. Hydrol. 13(2):40-60.

Harris, W. H. 1967. Stratification of fresh and salt water on barrier islands as a result of differences in sediment permeability. Water Resour. Res. 3(1):89-97.

Harris, W. H., and H. B. Wilder. 1964. Ground-water supply of Cape Hatteras National Seashore Recreational Area, Part 3, Rep. Invest. 4. N. C. Dep. Water Resour., Div. Ground Water, Raleigh, N. C.

Henry, H. H. 1964. Interface between salt water and fresh water in coastal aquifers, sea water in coastal aquifers. Water Supply Paper 1613C. U. S. Geol. Surv., Washington, D. C.

Hercules. 1966. Cellulose gum. Hercules Incorporated, Wilmington, Delaware.

Kashef, A. I. 1968. Diffusion and dispersion in porous media, salt water mounds in coastal aquifers, Rep. 11. Water Resour. Res. Inst., Univ. N. C., Raleigh, N. C.

Kimrey, J. O. 1960. Ground-water supply of Cape Hatteras National Seashore Recreational Area, Part 2, Rep. Invest. 2. N. C. Dep. Water Resour., Div. Ground Water, Raleigh, N. C.

Kimrey, J. O. 1961. Ground-water supply for the Dare Beaches Sanitary District, Rep. Invest. 3. N. C. Dep. Water Resour., Div. Ground Water, Raleigh, N. C.

Ligon, J. T., H. P. Johnson, and D. Kirkham. 1962. Unsteady-state drainage of fluid from a vertical column of porous material. J. Geophys. Res. 67:5199-5204.

Lloyd, O. B., Jr., and R. B. Dean. 1968. Ground-water supply of Cape Hatteras National Seashore Recreational Area, North Carolina, Part 6, Rep. Invest. 7. N. C. Dep. Water and Air Resour., Div. Ground Water, Raleigh, N. C.

Lloyd, O. B., Jr., and H. B. Wilder. 1968. Ground-water supply of Cape Hatteras National Seashore Recreational Area, North Carolina, Part 4, Rep. Invest. 5. N. C. Dep. Water and Air Resour., Div. Ground Water, Raleigh, N. C.

Polubarinova-Kochina, P. Ya. 1962. Theory of groundwater movement. Translated from Russion by J. M. R. DeWiest. Princeton Univ. Press, Princeton, N. J.

Rochester, E. W., Jr. and G. J. Kriz. 1968. Model study of boundary effects on ditch drainage. Irr. and Drainage Div. Amer. Soc. Civil Engr. 94:493-504.

Rochester, E. W., Jr. and G. J. Kriz. 1970. Ditch drainage of anisotropic nonhomogeneous porous media: a model study. Transactions of the ASAE 13(5):626-628.

Rubin, J. 1966. Theory of rainfall uptake by soils initially drier than their field capacity and its applications. Water Resour. Res. 2:739-749.

Snedecor, G. W., and W. G. Cochran. 1967. Statistical methods. The Iowa State Univ. Press, Ames, Iowa.

Taylor, D. A. 1948. Fundamentals of soil mechanics. John Wiley and Sons, Inc., N. Y.

Todd, D. K. 1959. Ground water hydrology. John Wiley and Sons, Inc., N. Y.

Van Driest, E. R. 1946. On dimensional analysis and the presentation of data in fluid flow problems. J. Appl. Mech. 13:A34-A40.

Verruijt, A. 1968. A note on the Ghyben-Herzberg formula. Bull. Intern. Ass. Sci. Hydrol. 13(4):43-46.

Wyrick, G. G., and R. B. Dean. 1968. Ground-water supply of Cape Hatteras National Seashore Recreational Area, North Carolina, Part 5, Rep. Invest. 6. N. C. Dep. Water and Air Resour., Div. Ground Water, Raleigh, N. C.

PUBLICATIONS RESULTING FROM PROJECT

1. Rochester, Eugene W., Jr. and George J. Kriz. 1970. Potable water availability on long oceanic islands. Journal of the Sanitary Engineering Div. Amer. Soc. Civil Engr. 96(SA5):1235-1248.

2. Rochester, Eugene W., Jr. and George J. Kriz. 1970. Ditch drainage of anisotropic nonhomogeneous porous media: a model study. Transactions of the ASAE 13(5):626-628.

3. Rochester, E. W., Jr. 1970. Potable water availability on long oceanic islands. Unpublished Ph.D. dissertation. North Carolina State University, Raleigh, N. C.

GLOSSARY OF SYMBOLS

Symbols

a	slope of discharge face (no units)
b	spacing between the parallel plates of the model (L)
c	time interval of infiltration in dimensionless form, $c = Kt/Wf$ (no units)
f	porosity of the soil (no units)
g	acceleration of gravity (L/T^2)
h	height above the impermeable layer of an open body of water (L)
h_1	height above the impermeable layer of an open body of water at the end of the flow region (L)
h_2	height above the impermeable layer of an open body of water at the end of the flow region (L)
i	unit vector in the x direction (no units)
I	depth of gallery below mean sea level (L)
j	unit vector in the z direction (no units)
K	hydraulic conductivity (L/T)
K_1	$K\alpha$ (L/T)
K_x	hydraulic conductivity in the x direction (L/T)
K_z	hydraulic conductivity in the z direction (L/T)
K*	equivalent isotropic hydraulic conductivity of anisotropic soil, $K^* = (K_x K_z)^{\frac{1}{2}}$ (L/T)
L	length of the flow region (L)
m	fluid mass (M)
M	model (no units)
n	number of values making up $\tilde{x}_1$ and $\tilde{x}_2$ (no units)
p	groundwater pressure (M/L^2)
P	prototype (no units)

Symbols

q	total discharge of fresh water into the ocean per unit thickness of the aquifer (L^2/T)
Q	pumping rate of fresh water per unit length (L^2/T)
Q_T	discharge from the model (L^3/T)
r	radial coordinate, $r = \sqrt{x^2 + (z - I)^2}$ (L)
R	rainfall intensity (L/T)
R_p	recharge parameter, $R_p = \lambda c/\gamma = (R/K)(t_c/t_\gamma)$ (no units)
R_v	rate of uniform vertical recharge per unit area ($L/T/L^2$)
s	standard deviation of sample of a normally distributed population (no units in this case)
$s_{1/4}$	standard deviation of $z_{i\ 1/4}/W$ (no units)
$s_{1/4}$	standard deviation of $z_{i\ 1/2}/W$ (no units)
$s_{(\bar{x}_1 - \bar{x}_2)}$	standard deviation of $(\bar{x}_1 - \bar{x}_2)$ (no units)
$S_0\ (z)$	unit step function defined as $S_0(z) = \begin{cases} 0 & z < 0 \\ 1 & z \geq 0 \end{cases}$ (no units)
t	time (T)
t_c	time period of rainfall (T)
t_γ	time period between rainfalls (T)
"t"	Student's distribution (no units)
V_r	Darcian velocity in the radial direction (L/T)
V_x	Darcian velocity in the x direction (L/T)
V_z	Darcian velocity in the z direction (L/T)
W	width of island at mean sea level (L)
x	horizontal Cartesian coordinate (L)

Symbols

x_i	horizontal coordinate perpendicular to island length and to z_i (L)
$\bar{x}_1$	sample mean (no units in this case)
$\bar{x}_2$	sample mean (no units in this case)
z	vertical Cartesian coordinate (L)
z_f	elevation of water table above sea level (L)
z_i	depth to the interface below sea level (L)
z^*	isotropic coordinate, $z^* = (K_x/K_z)^{\frac{1}{2}}z$(L)
α	$(\rho_s - \rho_f)/\rho_f$ (no units)
γ	cyclic time interval, $\gamma = Kt/Wf$ (no units)
Δx	incremental distance in horizontal x direction (L)
Δz	incremental distance in vertical direction (L)
Δm	fluid mass of a cube with sides Δx, 1, Δz (M)
λ	ratio of rainfall rate to hydraulic conductivity greater than zero (no units)
ν	kinematic viscosity (L^2/T)
μ_1	population mean (no units in this case)
μ_2	population mean (no units in this case)
ρ_f	density of fresh water (M/L^3)
ρ_s	density of salt water (M/L^3)
φ	Darcian velocity potential, $\varphi = -K(z + p/\rho_f g)$ (L^2/T)

A P P E N D I C E S

Appendix A. Experimental Results

Table 11. Effects of pumping from a gallery located at mean sea level at the island midpoint

R_p	γ	λ	$\frac{\rho_s}{\rho_f}$	$\frac{Q}{KW}$	$\frac{z_{i\ 0}}{W}$	$\frac{z_{i\ 1/4}}{W}$	$\frac{z_{i\ 1/2}}{W}$	$\frac{z_{f\ 1/4}}{W}$	$\frac{z_{f\ 1/2}}{W}$
0.00050	2	0.25	1.023	0	0.0125	0.0556	0.0667	0.00389	0.00389
				0.0000831	0.0111	0.0625	0.0695	0.00389	0.00444
				0.000173	0.0111	0.0625	0.0667	0.00389	0.00333
				0.000250	0.00972	0.0611	0.0639	0.00359	0.00306
				0.000302	0.00972	0.0611	0.0444	0.00278	0.00222
0.00075	2	0.25	1.023	0	0.00972	0.0722	0.0778	0.00416	0.00444
				0.000200	0.00972	0.0778	0.0834	0.00416	0.00406
				0.000256	0.00972	0.0806	0.0889	0.00359	0.00328
				0.000347	0.00972	0.0806	0.0889	0.00356	0.00300
				0.000412	0.0111	0.0778	0.0778	0.00333	0.00222
				0.000481	0.0111	0.0722	0.0667	0.00333	0.00195
				0.000537	0.0111	0.0722	0.0584	0.00306	0.00139
				0.000612	0.0111	0.0722	0.0444	0.00306	0.000834
				0.000666	0.0111	0.0667	0.0389	0.00306	0.000300
0.00200	4	1	1.023	0	0.0444	0.139	0.156	0.00416	0.00444
				0.000779	0.0444	0.139	0.156	0.00350	0.00234
				0.000988	0.0444	0.133	0.144	0.00333	0.00178
				0.00119	0.0444	0.133	0.144	0.00322	0.000300
				0.00124	0.0389	0.130	0.144	0.00345	0.000300
0.00200	4	0.25	1.023	0	0.0333	0.128	0.144	0.00416	0.00444
				0.000792	0.0333	0.128	0.144	0.00359	0.00195
				0.000972	0.0292	0.122	0.133	0.00359	0.00111
				0.00119	0.0264	0.121	0.125	0.00333	0.00111
				0.00125	0.0264	0.114	0.111	0.00306	0.000300

Table 11 (Continued)

R_p	γ	λ	$\frac{\rho_s}{\rho_f}$	$\frac{Q}{KW}$	$\frac{z_{i\ 0}}{W}$	$\frac{z_{i\ 1/4}}{W}$	$\frac{z_{i\ 1/2}}{W}$	$\frac{z_{f\ 1/4}}{W}$	$\frac{z_{f\ 1/2}}{W}$
0.00200	2	0.25	1.023	0	0.0333	0.122	0.144	0.00444	0.00500
				0.000690	0.0306	0.119	0.133	0.00359	0.00250
				0.000856	0.0250	0.111	0.111	0.00359	0.00195
				0.000947	0.0236	0.108	0.103	0.00333	0.00139
				0.00102	0.0194	0.101	0.0944	0.00306	0.000556
				0.00109	0.0194	0.100	0.0834	0.00306	0.000300
				0.00116	0.0194	0.0945	0.0778	0.00306	0.000300
0.00200	1	0.25	1.023	0	0.0306	0.117	0.133	0.00500	0.00500
				0.000692	0.0278	0.117	0.133	0.00472	0.00333
				0.000753	0.0278	0.117	0.125	0.00389	0.00278
				0.000846	0.0278	0.111	0.122	0.00389	0.00222
				0.00101	0.0278	0.111	0.111	0.00422	0.00189
				0.00116	0.0278	0.111	0.111	0.00344	0.00030
				0.00118	0.0278	0.111	0.111	0.00317	0.00030
0.00360	1	0.9	1.020	0	0.0945	0.225	0.251	0.00944	0.0100
				0.00200	0.0945	0.225	0.256	0.00556	0.00030
0.00480	1	0.9	1.020	0	0.139	0.261	0.289	0.00778	0.00834
				0.00200	0.136	0.264	0.289	0.00500	0.0030
				0.00250	0.139	0.267	0.289	0.00444	0.00030
0.00720	1	0.9	1.020	0	0.139	0.268	0.289	0.00722	0.0100
				0.00200	0.135	0.268	0.289	0.00666	0.00500
				0.00250	0.135	0.264	0.289	0.00500	0.00030
				0.00300	0.135	0.268	0.289	0.00500	0.00030
0.00720	0.5	0.9	1.020	0	0.150	0.283	0.300	0.00666	0.00500
				0.00200	0.150	0.283	0.306	0.00666	0.00500
				0.00250	0.153	0.283	0.306	0.00500	0.00030

Table 12. Effects of pumping from a gallery located below mean sea level (I/W = 5/180) at island midpoint

R_p	γ	λ	$\frac{\rho_s}{\rho_f}$	$\frac{Q}{KW}$	$\frac{z_{i\ 0}}{W}$	$\frac{z_{i\ 1/4}}{W}$	$\frac{z_{i\ 1/2}}{W}$	$\frac{z_{f\ 1/4}}{W}$	$\frac{z_{f\ 1/2}}{W}$
0.00200	4	0.25	1.023	0	0.0306	0.117	0.128	0.00444	0.00472
				0.000638	0.0278	0.117	0.122	0.00361	0.00334
				0.000894	0.0278	0.111	0.111	0.00333	0.00278
				0.00107		0.111	0.111	0.00333	0.00222
				0.00125	0.0222	0.104	0.0889	0.00333	0.00194
				0.00137	0.0222	0.0987	0.0722	0.00333	0.00167
				0.00152	0.0208	0.0945	0.0278	0.00333	0.00111

Table 13. Effects of pumping from a gallery located below mean sea level (I/W = 7/180) at island midpoint

R_p	γ	λ	$\frac{\rho_s}{\rho_f}$	$\frac{Q}{KW}$	$\frac{z_{i\ 0}}{W}$	$\frac{z_{i\ 1/4}}{W}$	$\frac{z_{i\ 1/2}}{W}$	$\frac{z_{f\ 1/4}}{W}$	$\frac{z_{f\ 1/2}}{W}$
0.00360	1	0.9	1.020	0	0.0945	0.228	0.256	0.00778	0.00889
				0.00200	0.119	0.228	0.247		
				0.00300	0.0840	0.179	0.167		
				0.00350	0.00834	0.142	0.0389	0.000556	-0.00278
0.00800	2	1	1.020	0	0.144	0.283	0.306	0.00695	0.00779
				0.00200	0.147	0.283	0.306	0.00500	0.00361
				0.00250	0.153	0.288	0.308	0.00722	0.00611
				0.00300	0.151	0.288	0.308	0.00333	0.00222
				0.00350	0.147	0.283	0.306		
				0.00450	0.147	0.283	0.306	0.00317	0
				0.00500	0.153	0.286	0.306	0.00122	-0.00444

Appendix B. Statistical Analysis

Standard Deviation of $z_{i\ 1/4}/W$ and $z_{i\ 1/2}/W$

The values of $z_{i\ 0}/W$ and $z_{i\ 1/4}/W$ which were presented in the Results are compiled from averages of two corresponding symmetrical values in the model. The value of $z_{i\ 1/2}/W$ was compiled from the midpoint location that had no corresponding symmetrical value. Both $z_{i\ 1/4}/W$ and $z_{i\ 1/2}/W$ were considered to be better indicators of changes in interface location than $z_{i\ 0}/W$ since the values of $z_{i\ 0}/W$ were of the same order of magnitude (1 cm) as the accuracy of the measurements. The value of $z_{i\ 1/4}/W$ was considered to be a better indicator of interface location than $z_{i\ 1/2}/W$ because $z_{i\ 1/4}/W$ was an average of two values and because $z_{i\ 1/2}$ was hard to determine due to dispersion of the fluids. The fluid dispersion at $z_{i\ 1/2}$ was caused by repeated variation of the interface location at that point.

The replicated results are presented in Table 14.

Table 14. Location of interface for two replicated tests

R_p	Rep	$z_{i\ 0}/W$	$z_{i\ 1/4}/W$	$z_{i\ 1/2}/W$
0.00200	1	0.0333	0.128	0.144
	2	0.0306	0.117	0.128
0.00360	1	0.0945	0.225	0.251
	2	0.0945	0.228	0.256

The pooled standard deviation for $z_{i\ 1/4}/W$, $s_{1/4}$, and for $z_{i\ 1/2}/W$, $s_{1/2}$, is 0.00570 and 0.00838, respectively (Snedecor and Cochran (1967)).

Significance of Varying Infiltration Rates on Interface Location as Presented in Table 2.

Snedecor and Cochran (1967) presented a method of comparing two independent samples to determine if these samples were obtained from the same population (treatment). This comparison was made with the Student's "t" distribution which is defined as

$$"t" = \frac{(\bar{x}_1 - \bar{x}_2) - (\mu_1 - \mu_2)}{s_{(\bar{x}_1 - \bar{x}_2)}}, \qquad (45)$$

where

$s_{(\bar{x}_1 - \bar{x}_2)} = \sqrt{\frac{2s^2}{n}}$ is the standard deviation of $(\bar{x}_1 - \bar{x}_2)$,

n = the number of values composing $\bar{x}_1$ and $\bar{x}_2$,

s = the standard deviation of $\bar{x}_1$ and $\bar{x}_2$,

"t" = Student's distributions,

$\bar{x}_1$ and $\bar{x}_2$ = the independent sample means,

and

μ_1 and μ_2 = the population means.

The hypothesis made was that there was no effect on interface location due to infiltration rate variation as presented in Table 2. Thus, the average values of $z_{i\ 1/4}/W$ for the two infiltration rates presented in Table 2 were hypothesized to be equal, i.e., $\mu_1 = \mu_2$. The variance $s = s_{1/4}$ was assumed to be that which was calculated in Table 7, i.e., $s_{1/4} = 0.00570$. The deviation of the difference between the two sample values is

$$s_{(\bar{x}_1 - \bar{x}_2)} = \sqrt{\frac{2s^2}{n}} = 0.00806 \qquad (46)$$

The value of "t" is

$$"t" = \frac{(0.139 - 0.128) - (0)}{0.00806} = 1.35.$$

According to Student's distribution (s having 1^{o} of freedom, a value of "t" greater than 12.7 (significance level of 5 percent) is needed to reject the hypothesis that no effect on interface location due to variation in the infiltration rate exists. Thus, the hypothesis is accepted. Although the statistical deviation from the hypothesis was not significant, the number of replications was so small that this result gives only a weak confirmation. However, the infiltration rate can be ignored as a dominant factor affecting the location of the interface.

Significance of Varying Cycle Duration (Interval of "Fresh-Water" Addition) on Interface Location as Presented in Table 3

The Student's "t" distribution was used to determine any significant differences in the interface locations as a result of the various cycle durations employed. The standard deviation of the difference between two samples was determined in equation 46 to be $s_{(\bar{x}_1 - \bar{x}_2)} = 0.00806$. The value of "t" is

$$"t" = \frac{(0.128 - 0.117) - (0)}{0.00806} = 1.36$$

for the difference between $\gamma = 4$ and $\gamma = 1$. The hypothesis that $\mu_1 = \mu_2$, i.e., no effect from varying cycle duration, was made. The value of "t" is much less than the 12.7 needed to indicate a significant

difference in the values of interface location. Again, the hypothesis that no difference in interface location exists is accepted with the reservation that the number of duplications is small and that confirmation is weak. Because the infiltration interval was varied by a factor of four and no significant variation in interface location resulted, the infiltration interval was not a significant factor in determining interface location.